

Simulation of Anterior Cruciate Ligament Injury and Reconstruction Using a 3D Finite Element Knee Joint Model

by

Jeremy F. Suggs

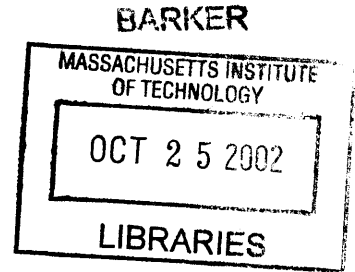
B.S., Mechanical Engineering
University of Pittsburgh, 1999

Submitted to the Department of Mechanical Engineering
in Partial Fulfillment of the Requirements for the Degree of
Master of Science in Mechanical Engineering

at the

Massachusetts Institute of Technology


June 2002

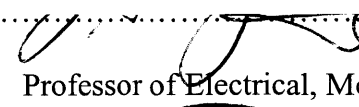


© 2002 Massachusetts Institute of Technology
All rights reserved

The author hereby grants to MIT permission to reproduce and to distribute publicly paper and electronic copies of this thesis document in whole or in part.

Signature of Author..... 
Department of Mechanical Engineering
May 24, 2002

Certified by..... 
Guoan Li
Lecturer
Thesis Advisor

Certified by..... 
Alan J. Grodzinsky
Professor of Electrical, Mechanical, and Bioengineering
Reader

Accepted by.....
Ain Sonin
Chairman, Department Committee on Graduate Students

Simulation of Anterior Cruciate Ligament Injury and Reconstruction Using a 3D Finite Element Knee Joint Model

by

Jeremy F. Suggs

Submitted to the Department of Mechanical Engineering
on May 24, 2002 in partial fulfillment of the
requirements for the Degree of
Master of Science in Mechanical Engineering

ABSTRACT

A three dimensional computational knee joint model was utilized in simulating injury to the ACL and ACL reconstruction. The model was constructed and optimized using MR images and experimental data from the same knee. The model was validated by comparing its behavior to kinematic and kinetic data found in literature. The focus of the simulation was a parametric study of the effect variations in the stiffness of the ACL or graft material has on knee joint function

The stiffness of the ACL was reduced by varying degrees to simulate partial ACL injury and complete ACL rupture. The behavior of the ACL deficient knee was analyzed under a simulated quadriceps load. Stiffness reduction of the ACL did have a considerable effect on knee joint function, although the results show that an injured ACL can still provide a majority of the stability provided by an intact ACL.

ACL reconstruction was simulated using grafts with material properties similar to those of grafts most often used today. The results show that current reconstruction techniques, especially when high initial graft tensions are used, are likely to produce abnormal knee kinematics and kinetics. The graft fixation sites should be chosen such that the graft behavior matches that of the intact ACL.

Thesis Supervisor: Guoan Li
Title: Lecturer

Biographical Note

INSTITUTIONS:

University of Pittsburgh, Pittsburgh, PA (1995 – 1999)

- Byrd Scholar (1995 – 1999)
- University Scholar (1997 – 1999)
- Pi Tau Sigma
- First Prize in ASME IMECE B.S. Paper Competition, Bio Division (1999)
- B.S. in Mechanical Engineering (December, 1999)

Massachusetts Institute of Technology, Cambridge, MA (2000 -)

- National Science Foundation Fellow (2000 -)
- Leventhal Fellow (2000 – 2001)
- Second Prize in ASME IMECE M.S. Paper Competition, Bio Division (2001)

PUBLICATIONS:

1. Li, G., J.F. Suggs, and T. Gill, *The Effect of ACL Injury on Knee Joint Function under Simulated Muscle Load*. Ann Biomed Eng, In press.
2. Suggs, J., G. Li, and C. Wang, *The Effect of Graft Stiffness on Knee Joint Biomechanics after ACL Reconstruction - A 3D Computational Simulation*. Clin Biomech (Bristol, Avon), Submitted.

1. Introduction

1.1 Objective

Of the ligaments in the knee, the anterior cruciate ligament (ACL) is the most frequently injured. Feagin has estimated over 100,000 anterior cruciate ligament (ACL) injuries per year just from ski accidents [3]. Other studies report ACL injury rates of 0.24 to 0.34 per 1000 people a year (70,000 to 100,000 people/yr) [4, 5]. A study of army aviators found that there were 0.52 ACL injuries requiring reconstruction per 1000 aviators per year, 76% of which occurred during sporting activities [6]. ACL deficiency can lead to cartilage damage and degeneration [4, 7, 8]. Ferretti et al and Hawkins et al found that ACL deficient subjects who developed posttraumatic osteoarthritis were 15 to 20 years younger than uninjured subjects who developed primary osteoarthritis [9, 10].

ACL reconstruction is a common procedure performed to restore anterior knee stability [11]. While current techniques are successful in restoring knee stability, they do not necessarily restore intact kinematics or prevent the early joint degeneration seen in ACL deficient patients. Clinical studies have indicated that 38% of ACL reconstructions have abnormal results [12]. Daniel et al reported a greater incidence of joint degeneration in ACL reconstructed knees than in injured knees that did not undergo reconstruction [4]. One must conclude, then, that despite the abundance of informative research on many factors that influence the outcome of ACL reconstructions, there are still improvements to be made.

A better understanding of the effects various factors have on the outcome of ACL reconstruction is required in order to improve current reconstruction techniques. Validated computational models of the knee are an advantageous method for bolstering our knowledge of the intricacies of ACL reconstruction. In this work, a 3-D computational knee joint model, properly validated through comparison with experimental data, was used to analyze the effect of ACL and graft stiffness on knee kinematics and kinetics under simulated anterior-posterior tibial loads and quadriceps loads. The information obtained in this work will help guide investigators and surgeons to an optimal ACL reconstruction.

1.2 Clinical Outcomes of ACL Reconstruction

ACL reconstruction is performed primarily to restore anterior stability to the knee after injury to the ACL. Without the presence of the ACL, the tibia is liable slip anteriorly from under the femur during certain movements such as cutting or side-stepping. A secondary goal of ACL reconstruction is to prevent early degeneration of the articular cartilage of the knee, which has been observed in ACL injured knees treated non-surgically [4, 8]. Currently, ACL reconstruction is most often performed using a bone-patellar tendon-bone graft (BPTB) or a hamstring tendon graft [8], because these grafts can withstand the loads experienced by the intact ACL [2].

Many long-term clinical studies have concluded that current ACL reconstructions are able to restore overall anterior tibial stability [13-15]. Plancher et al followed 75 knees for an average of 55 months [13]. The mean difference in anterior laxity between the reconstructed knee and the contralateral, uninjured knee measured by KT-1000 was 1.4 mm, and no patients reported any giving way. Grontvedt et al performed a study including 48 patients who underwent ACL reconstruction with a BPTB graft with an average follow up time of five years [14]. At final follow up, 79% of the patients had a side-to-side laxity difference of less than 3 mm, and the remaining 21% had a side-to-side difference of less than 5 mm. Aglietti et al compared BPTB and doubled semetendinosus and gracilis (DST/G) reconstructions for a minimum follow-up period of five years [15]. Eighty three percent and 70 percent of the BPTB reconstructed knees and DST/G reconstructed knees, respectively, had a side-to-side laxity difference of less than 5mm, although this difference was not statistically significant.

While ACL reconstruction has been shown to restore anterior knee stability, studies have also shown that reconstruction does not necessarily guarantee the absence of early joint degeneration [16-21]. Deehan et al reported that 90% of a population of 90 knees were normal or nearly normal at five-year follow-up[16]. They conclude that reconstruction can prevent degeneration when the menisci are undamaged at the time of surgery. In a study of forty-four patients who had ACL reconstruction using a 10mm BPTB, Aglietti et al found moderate radiographic changes in 18% of the subjects, but there was a positive correlation between radiographic changes and meniscectomy [17]. Jomha et al reported radiographic changes even in knees with intact menisci, although

degenerative changes were more severe when a meniscectomy was performed or the reconstruction was done more than 12 weeks after the injury [18]. Jarvela et al did a retrospective study of 100 patients who underwent ACL reconstruction with a BPTB graft [20]. At an average follow-up of seven years, 47 patients had degeneration in the patellofemoral joint, even though only 18 patients had degeneration in the medial tibiofemoral joint, and only 14 patients had degeneration in the lateral tibiofemoral joint.

These results show that the primary goal of restoring anterior knee stability is being met by current reconstructions. Giving way of reconstructed knees is almost non-existent, and the vast majority of reconstructed knees behave in an at least near normal fashion during anterior drawer testing. Despite the improvements in knee function offered by current reconstructions, joint degeneration still occurs in the long term. Abnormal loading of the cartilage, which can be caused by abnormal knee function, has been suggested as an etiology of joint degeneration [22]. The fact that joint degeneration is not being prevented indicates that current reconstruction techniques may not completely restoring normal knee function.

1.3 Biomechanical Analysis

1.3.1 Intact and ACL Deficient Knee Kinematics and ACL Force

In order to determine the best possible reconstruction technique, it is necessary to know how the intact knee behaves. It is also advantageous to know what effect injury to the ACL has on the behavior of the knee joint. To this end, many investigators have used various techniques to gain information on how the intact and injured knee functions [23-40]. Since the in vivo loads experienced by the knee during daily activities are unknown, in vitro studies typically analyzed knee function during passive motion or under anterior-posterior (AP) loads of approximately 100 N. These loads are low compared to the loads experienced by the knee in vivo, which are estimated to be up to several times body weight. However, the magnitude of the loads used in testing is generally limited by the testing system.

AP laxity testing has also been done in vivo. Daniel et al determined the AP laxity of 338 uninjured subjects and 89 subjects with unilateral ACL tear [27]. Knee laxity was measured using a clinical tool called the KT-2000, which holds the knee at

about 20° of flexion and applies an 89 N anterior or posterior drawer load. The mean ATT of the uninjured and injured knees was 5.7±1.9 mm and 13.0±3.5 mm, respectively.

Fukubayashi et al used a six degree of freedom (DOF) apparatus to determine the AP laxity of the knee joint under 100 N loads [23]. The maximum anterior tibial translation (ATT) of 7.0 mm occurred with the knee at 30° of flexion. They found the tibia to rotate internally and externally under the anterior and posterior loads, respectively. The maximum internal tibial rotation (ITR) of almost 10° occurred with the knee between 30 and 45° of flexion. When tibial rotation was constrained, tibial translation was approximately 25% less than when the tibia was allowed to rotate freely for all flexion angles. When the ACL was cut, ATT increased to almost 2.5 times that of the intact ATT, and ITR practically disappeared, yet tibial movement under posterior loading was unaffected.

The results from the study by Fukubayashi et al mentioned above suggest that the ACL causes internal tibial rotation. While most agree that the ACL affects tibial rotation, other investigators have proposed that the ACL resists internal tibial rotation rather than causes rotation [36, 41-43]. Andriacchi et al measured in vivo motion of the knee joint during gait by tracking the motion of point clusters attached to the thigh and shank [36, 44]. The AP motion of the ACL deficient knee during the gait cycle was surprisingly similar to that of the intact knee. However, the tibia of the ACL deficient knee was significantly internally rotated compared to the intact position. The difference in conclusions about the role of the ACL in tibial rotation among investigators is probably due to different loading conditions. If an anterior tibial force is applied medial to the tibial ACL insertion, it will produce an external torque when coupled with the ACL force. On the other hand, if the anterior tibial force is applied lateral to the tibial ACL insertion, it will produce an internal tibial torque when coupled with the ACL force. Thus, the role the ACL plays in tibial rotation is load dependent.

There have also been investigations into the tension carried by the ACL [29, 45]. Woo et al developed a 6 DOF robotic testing system to measure the forces in the anteromedial (AM) and posterolateral (PL) bundles of the ACL under anterior tibial loads ranging from 22 to 110 N [24]. The forces in the AM bundle varied from 32.6±13.3 N at 0° of flexion to 47.4±34.2 N at 60° of flexion. The forces in the PL bundle varied from

4.6±2.5 N at 90° to 13.7±8.1 N at 0°. The magnitude of the force in the AM bundle was not significantly affected by the flexion angle. The effect of flexion angle on the total ACL force was similar to that on the PL bundle force. Li et al also used a robotic testing system to determine the ACL force under simulated muscle loads [29]. The in-situ force in the ACL under a 200 N quadriceps load was found to increase from 27.8±9.3 N at full extension to a maximum of 44.9±13.8 N at 15° of flexion and then decrease to 10 N beyond 60° of flexion. The in-situ force at 15° was significantly higher than that at other flexion angles. The addition of a hamstring load of 80 N significantly reduced the in-situ force in the ACL at 15, 30 and 60° of flexion by 30, 43, and 44%, respectively. The data also suggest that hamstring co-contraction with quadriceps is effective in reducing excessive forces in the ACL particularly between 15 and 60° of knee flexion.

1.3.2 Factors Affecting Reconstruction, Reconstructed Kinematics and Graft Force

Currently, bone patellar tendon bone (BPTB) grafts or semitendinosus and gracilis (ST/G) are most often used to reconstruct the ACL [8]. Several investigators have performed long-term clinical studies to determine if there are differences in the outcomes of these reconstructions [15, 21, 46-49]. Marder et al [46], Aglietti et al [15, 47], and Eriksson et al [48] compared BPTB and quadrupled semitendinosus and gracilis (QST/G) grafts and found no difference between the two. Otero and Hutcheson [49] and O'Neill [21] compared BPTB and doubled semitendinosus and gracilis (DST/G) grafts. Otero and Hutcheson found the BPTB graft to provide significantly greater stability than the DST/G graft. O'Neill did not find any significant difference in the stability of the two grafts but did find differences with regard to muscle strength. The knees reconstructed with BPTB grafts were more likely to have deficits in quadriceps strength, while knees reconstructed with DST/G grafts were more likely to have deficits in hamstring strength. The choice of graft did not have an effect on the rate of degenerative arthritis.

Clinically, the success of an ACL reconstruction in restoring knee function is most often measured by the amount of anterior tibial laxity under an anterior tibial load of approximately 90 N [13-15, 21, 46-49]. As discussed in Section 1.1.2, clinical investigators have reported on the AP laxity of reconstructed knees at some time after surgery, usually around five years. Unfortunately, these studies only measure AP laxity

and not tibial rotation, which is also an important factor in knee motion. Furthermore, measurements are only taken at one flexion angle, typically 20 to 30°, so there is question as to how the grafts behave at other flexion angles. The behavior of the reconstructed knee immediately after surgery is generally not measured.

To gain more knowledge of the behavior of ACL reconstructed knees, investigators have turned to cadaveric experiments similar to those used in analyzing intact knees [1, 23, 25, 27, 29, 33, 34, 40, 43, 45, 50-70]. Studies have reported on the effect of initial graft tension, graft placement, fixation location, fixation technique, and knee position during fixation.

The initial tension in the graft upon fixation is one of the most important factors in ACL reconstruction [52, 55, 62, 71]. Burks and Leland determined the initial graft tension necessary for three different graft types to provide anterior laxity equal to that of the intact knee as measured by a KT 1000 (89 N) [52]. They suggested initial tensions of 16, 38, and 60 N for 10 mm BPTB, doubled semitendinosus, and 3 cm iliotibial band grafts, respectively. Yasuda et al performed an in vivo study of ACL reconstruction using QST/G grafts in series with polyester tapes [71]. Three initial graft tensions of 20, 40, and 80 N were used in the reconstruction. Knees reconstructed with an 80 N initial tension were found to have laxity closest to the uninjured contralateral knees.

Many of these studies have shown that ACL reconstruction may result in abnormal knee kinematics [55, 72, 73]. Bylski-Austrow et al performed ACL reconstructions on cadaver knees using a graft system with stiffness similar to the intact ACL [72]. The graft was fixed in all combinations of 0° and 30° of flexion with initial tensions of 22 and 44 N. When tested under a 100 N anterior tibial load, the knees were found to be over-constrained when the graft was fixed at 30°. Fleming et al also performed ACL reconstructions on cadaver knees using a graft with stiffness similar to the ACL [55]. The grafts were fixed with initial tensions of 0, 0, 18, and 27 N with the knee in 30° of flexion. The knee kinematics was found to be over-constrained under a 150 N anterior tibial load. Since BPTB and hamstring grafts are stiffer than the ACL, these studies suggest that reconstructions using BPTB or hamstring grafts may over-constrain the knee ACL [2, 54, 74, 75].

Tashman et al used a cine-radiographic method to measure in vivo kinematics in intact and reconstructed knees with BPTB or quadrupled semitendinosus grafts [37]. Tantalum beads were implanted in the tibia and femur, and their motion was tracked during downhill treadmill running and one-legged forward hopping. This study found that anterior-posterior motion was restored, but the tibia of the reconstructed knee was externally rotated compared to the intact knee. Andriacchi et al found ACL deficient knees to have significant internal rotation compared to intact knees during gait [36]. These studies also suggest that current reconstruction techniques may overconstrain the knee.

1.4 Computational Knee Joint Models

1.4.1 Motivation for Modeling

Current ACL reconstruction techniques are a proven method for restoring anterior knee stability [13-15]. However, these techniques have been shown to be inconsistent in restoring normal knee kinematics [37, 38, 55, 72, 73] and preventing early joint degeneration [16-21]. Many investigators have studied the effect of various parameters in ACL reconstruction on the behavior of a reconstructed knee in order to improve current techniques [51, 52, 55, 61-63, 69, 71, 72, 76]. These experiments are limited in their scope and magnitude for several reasons. Human specimens for in-vitro studies are expensive and can be tested for a limited amount of time before tissue degradation makes the results irrelevant. It is difficult to control the various parameters that affect ACL reconstruction. It is also difficult to apply a wide range of loading conditions in most in vitro tests, although this issue is being addressed by developments such as robotic testing systems [24, 77].

The limitations of these types of experiments make a validated computational knee joint model an attractive alternative for parametric studies. Models are much cheaper and can be used indefinitely. The parameters of interest can be controlled to practically any accuracy desired by the user. Future simulated experiments are unaffected by any experiments done previously, and experiments can be completed in a fraction of the time it takes to in vitro testing. The key to use of a computational model is

proper validation of the model. A model should be validated by comparing its results to experimental results obtained over a range of loading conditions and magnitudes.

1.4.2 Previous Models

Mathematical knee models have been reported as far back as 1904 [35, 78-85]. Wismans et al developed one of the first models of great similarity to the one utilized in this work [82]. The geometry of the model was measured from a cadaver specimen using a dial gauge. The ligaments and capsule were represented by 7 quadratic spring elements. Ligament stiffness data was obtained from Trent et al [86]. The bone and cartilage were assumed to be rigid. The menisci and friction were ignored.

Andriacchi et al developed a knee joint that did model deformation of the tibiofemoral cartilage [35]. The bone was assumed to be rigid, and the menisci were represented by two shear beam elements. The ligaments were modeled as multi-bundle structures using 21 linear spring elements. The cartilage was represented by ten 8-node hydrostatic elements each having four nodes attached to the femur and four nodes attached to the tibia.

A model developed by Essinger et al included the tibia, femur and patella [83]. The femur, patella, and patellar tendon, which connects the tibia and patella, were assumed to be rigid, while the tibia was allowed to deform. All four major ligaments were represented by quadratic spring elements, each ligament except the LCL having two elements. The menisci and friction were ignored.

The model applied here is probably most similar to the model developed by Blankevoort et al [84, 85]. The model included the tibia and femur, which were assumed to be rigid, with deformable cartilage on the articulating surfaces. The cartilage is assumed to be linear elastic. The ligaments and capsule were represented by 12 quadratic spring elements. The menisci were not included in the model. The model geometry was obtained using stereophotogrammetric and Roentgenstereophotogrammetric methods.

The knee joint model utilized in this work has several advantages over these previous models. First, only Andriacchi et al included a representation of the menisci. The model in this work included elements representing the menisci and also modeled cartilage deformation as deformation of two distinct layers, which was not done by any of

these models. Only Blankevoort et al used an optimization procedure to increase the accuracy of the model prior to validation. The initial strains of the ligaments were adjusted until model predictions matched experimental data obtained from a knee tested under a ± 3 Nm tibial torque. The model in this work was optimized to match experimental data collected under independent anterior-posterior tibial loads of ± 134 N and internal-external tibial moments of ± 10 Nm. The greatest strength of this model is its rigorous validation. The previous models were validated by comparing the kinematics predicted by the model to those obtained experimentally. The model in this work was validated by not only comparing the kinematics predicted by the model to experimental data under a wide range of loading conditions, but also by comparing forces in the ligaments predicted by the model to experimental data found in literature.

2. Materials and Methods

2.1 Model Construction

2.1.1 MR Imaging and Digitization

A 3D finite element model of a left cadaveric knee specimen (male, 62 years old) was constructed using MR images. The knee was scanned in full flexion on a 1.5 Tesla magnet (Signa Horizon, GE, Milwaukee, Wisconsin). The images were acquired in the sagittal plane using a fat suppressed gradient echo sequence. A cubic volume measuring approximately 140 mm on a side was scanned with 0.7 mm between the images. There were 512 pixels along the height and width of each image. After the images were acquired, the contours of the tibia, femur, patella, and articular cartilage in each MR image were digitized using available image software. (Figure 1)

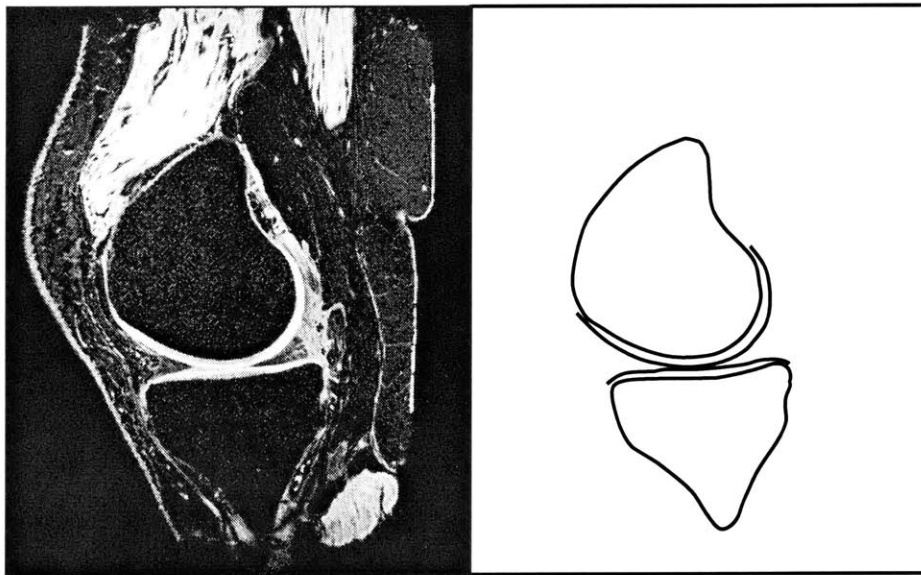


Figure 1. Outlines of the bone and cartilage are made from MR images of the knee joint.

The contours were imported into MSC/Patran® (MSC Software Corp., Santa Ana, CA) where they were used to create surfaces and volumes representing the bone and cartilage. The insertions of the ACL, posterior cruciate ligament (PCL), medial collateral ligament (MCL) including deep capsular fibers, and lateral collateral ligament (LCL) of the

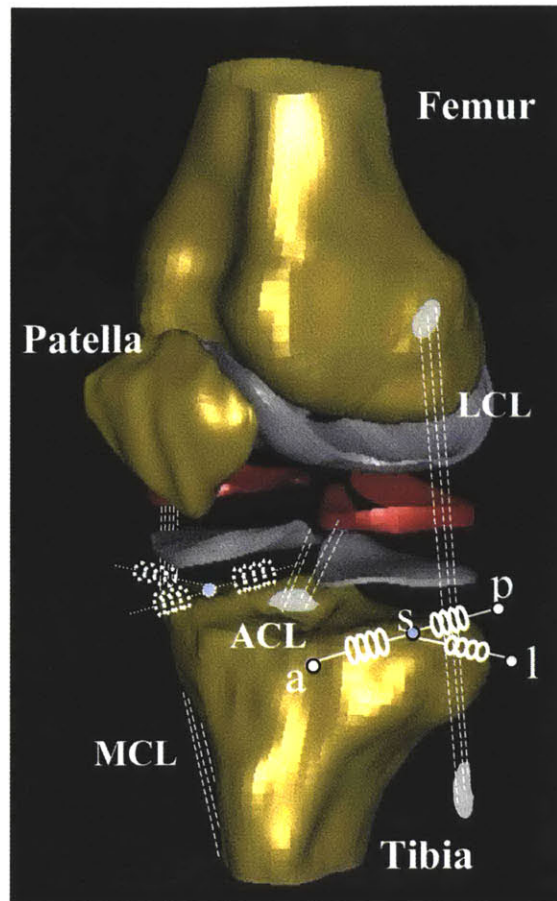


Figure 2. Knee model created from MR images including the femur, patella, and tibia, the tibiofemoral articular cartilage, and the ligaments (PCL not shown). The position of the menisci, shown in red, was represented by nonlinear compressive springs. On the lateral side, **a-s** represents the anterior compressive spring, **p-s** the posterior spring, and **s-l** the lateral spring. Points **a**, **p**, and **l** were fixed to the tibia while point **s** was fixed to the femur. There are similarly 3 springs used at the medial side.

cadaver specimen were digitized along with bony landmarks using Microscribe® (Immersion Corp., San Jose, CA). The ligament insertions were also imported into MSC/Patran® and aligned on the model using the bony landmarks [32]. (Figure 2)

2.1.2 Material Properties and Constitutive Modeling

Cartilage material properties are dependent on the time scale of the event in question (impact vs. long term). For impact type loading, the reported modulus and Poisson's ratio are 5 to 15 MPa and approximately 0.5, respectively. For long term events, the modulus is on the order of 1 MPa, and Poisson's ratio is 0.0 to 0.4. The cartilage in the model had a Young's Modulus of 5 MPa and a Poisson's Ratio of 0.45

[32, 84]. These values were chosen to reflect cartilage behavior during testing or normal walking, which have time scales between impact and long term events. In the analysis of the contact between the cartilage layers, both layers were allowed to deform. A more complete discussion of the contact modeling is given in Appendix A. Reported values for the Young's Modulus of human cortical bone in the femur and tibia range from 5 to 25 GPa, and values for cancellous bone range from 4 to 18 Gpa [87]. Given the fact that the modulus of cartilage is only 5 MPa, and the modulus of the ligaments is around only 350 MPa [74], the bone was assumed to be rigid in the model.

The ligaments were modeled as multi-bundle structures [74, 84, 88]. The ACL was modeled as having two bundles, the anterior-medial (AM) bundle and the posterior-lateral (PL) bundle. The AM bundle was represented by two non-linear tensile spring elements, an anterior element and a medial element. The PL bundle was also represented by two spring elements, a posterior element and a lateral element. So, the ACL was represented by a total of four elements. In a similar fashion, the PCL was represented four elements, the LCL by three elements, and the MCL, including deep (capsular) fibers, by five elements.

The force-strain relation is given by a piece-wise function adopted from the literature [32, 84]:

$$f = \begin{cases} 0, & \varepsilon < 0 \\ \frac{k\varepsilon^2}{4\varepsilon_l}, & 0 \leq \varepsilon \leq 2\varepsilon_l \\ k(\varepsilon - \varepsilon_l), & \varepsilon > 2\varepsilon_l \end{cases} \quad (1)$$

The variable f represents the force in the ligament, k is the stiffness parameter or axial rigidity, ε_l is a strain parameter, and ε is the strain, which is given by:

$$\varepsilon = \frac{l - l_o}{l_o} \quad (2)$$

where l is the deformed length, and l_o is the zero-load length. The strain parameter ε_l in Equation (1) is used to describe the transition of the ligament behavior from the non-linear, toe region to the linear region and is assumed to be 0.03 [32, 84]. When the bundle strain is less than zero (in compression), the bundle carries no load. In other

words, the ligaments only carry load in tension. When the bundle strain is less than $2\varepsilon_t$, the bundle force is given by a quadratic function of the strain. When the bundle strain is greater than $2\varepsilon_t$, the bundle force is given by a linear function of the strain (Eq. 1). This constitutive relation is very capable of representing the load-elongation behavior of both ligaments and grafts as shown in Figure 3.

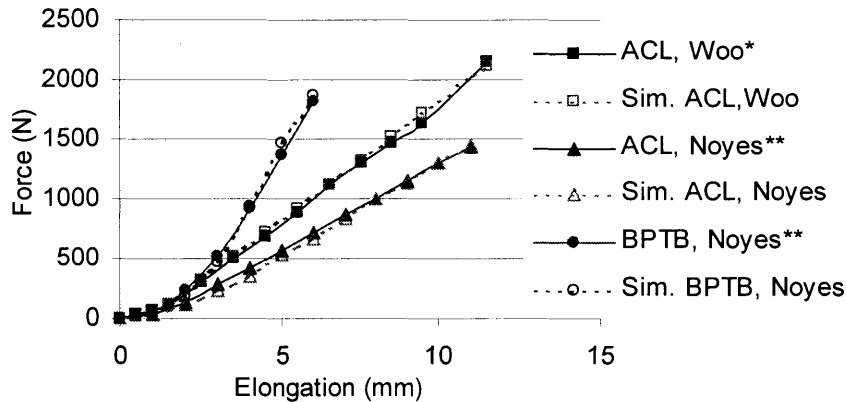


Figure 3. Comparison of the piece-wise function to typical ACL and BPTB graft force-elongation curves.

*Woo et al., 1991 [1]

** Noyes et al., 1984 [2]

There have been many studies evaluating the material properties of the knee ligaments and grafts used to replace the ACL in ACL reconstruction [2, 74, 75, 86]. A good estimate of the ligament and graft stiffness is needed in order to construct a valid model, but there appears to be wide variations in the reported stiffness values of the ligaments and grafts. There are a few ways to report the “stiffness” of a material. A common characterization of a ligament’s stiffness is the traditional “structural stiffness” (SS), which is the force generated in the ligament per unit elongation. A second characterization of a ligament’s stiffness, which is also commonly used, is the elastic or Young’s modulus, which is the force generated per unit strain per unit cross-sectional area. The modulus is a pure measure of a material’s stiffness and is independent of a specimen’s dimensions. Previous computational knee models have characterized the ligaments stiffness by what is often referred to as the stiffness parameter, which is the force generated per unit strain and is represented by k in Equation (1). For strains in the linear region of the force-strain curve, the stiffness parameter corresponds to the axial

rigidity of the ligament. This stiffness characterization is convenient for computational knee models, because the rigidity is independent of the zero-load length, and the cross-sectional area of the ligament or graft does not have to be defined explicitly. The rigidity is equal to the structural stiffness divided by the zero-load length and is equal to the modulus multiplied by the cross-sectional area.

The stiffness of the intact ligaments in our model were based mainly on the work of Blankevoort et al. [84]. The stiffness data in that study was based on a combination of work by Danylchuk [89], Wismans et al [82], Andriacchi et al [35], and Butler et al [74]. Andriacchi combined stiffness data from Trent et al [86] with data from Girgis et al [90] and determined stiffness values that were slightly higher than those of Wismans. Danylchuk found the areas of the ACL, PCL, and MCL to be 35, 58, and 24 mm², respectively. Butler et al found an average modulus for the ACL, PCL and LCL of 345 MPa (N/mm²). Assuming this average modulus to hold for the MCL also, Blankevoort et al calculated rigidities for the ACL, PCL, and MCL, which were higher than those determined by Andriacchi et al (Table I)

Table 1 lists rigidity values adapted from a chart from Blankevoort et al [84], along with some data from other work. Noyes et al determined the stiffness of the ACL and several graft materials [2]. The values varied greatly depending on if the strain was calculated referring to the separation of the grips holding the specimen (grip to grip) or measured with strain gauges (local). The gauges measured a much lower strain and thus a much higher stiffness than the grip-to-grip measurements. Butler et al measured the modulus of the ACL, PCL, and LCL, and the patellar tendon (PT) [74]. Axial rigidities for the ACL and central third BPTB graft were calculated by combining the moduli of the ACL (not including the moduli of the PCL or LCL) and PT with area measurements by Noyes et al (Table 1). The calculated ACL rigidity was comparable to the value obtained by Blankevoort et al combining data from Danylchuk and Butler et al. The calculated BPTB rigidity was comparable to the local measurements of Noyes et al. The axial rigidities for the intact ligaments in our model were distributed evenly over all the elements of each ligament.

Table 1: Comparison of Axial Rigidities (N) for ligaments and ACL grafts found in literature

Bundle/ Graft	Trent (1976)	Wismans (1980)	Andriacchi (1983)	Danylchuk- Butler (1975-1986)	Noyes, Local (1984)	Noyes, Grip to Grip (1984)	Hamner (1999)	Butler (1986)	Butler (1992)
ACL	3041	3000	7200	12075	-	4914	-	13320	-
AMB	-	-	-	-	-	-	-	-	3142
ALB	-	-	-	-	-	-	-	-	3173
PB	-	-	-	-	-	-	-	-	3439
PCL	4483	4500	14300	20010	-	-	-	-	-
LCL	3051	3000	7300	-	-	-	-	-	-
MCL	5160	8000	8200	8280	-	-	-	-	-
CM	-	1000	-	-	-	-	-	-	-
CL	-	1000	-	-	-	-	-	-	-
Central 3rd PT, 14mm	-	-	-	-	31016	18427	-	32155	-
Medial 3rd PT, 15mm	-	-	-	-	-	17485	-	-	-
Semi- tendinosus (1 strand)	-	-	-	-	15051	5022	6390	-	-
Gracilis (1 strand)	-	-	-	-	12987	4597.21	4800	-	-
Gracilis and Semi- tendinosus (4 strands)	-	-	-	-	-	-	23280	-	-

AMB = Anterior medial bundle of the ACL, ALB = Anterior lateral bundle of the ACL

PB = Posterior bundle of the ACL,

CL = Lateral posterior capsule, CM = Medial posterior capsule

It is unclear whether Noyes et al. used single strands or double strands for the semitendinosus tests and gracilis tests.

The menisci were modeled as non-linear compressive springs distributed in the medial-lateral and anterior-posterior directions as shown in Figure 2 (compressive springs). They followed a force-strain relation similar in form to that of the ligaments with the only difference being force was generated with compression (negative strains) instead of tension.

The last step in building the knee model was defining coordinate systems for the tibia and femur. The two coordinate systems were defined at the same position with the knee in full extension, so in effect, only one coordinate system needed to be defined initially. The origin of the coordinate system, or knee center, was defined as the midpoint

of the transepicondylar line (Figure 4). The medial-lateral (z) axis was defined as the transepicondylar line, the proximal-distal (y) axis was defined as the longitudinal axis of the tibia, and the anterior-posterior (x) axis was defined as the cross product of the y and z axes. This coordinate system definition gives the initial position of the tibial and femoral coordinate systems at full extension. These coordinate systems were fixed in their respective bones, and relative motion between the tibia and femur was measured as the relative motion between the tibial and femoral coordinate systems.

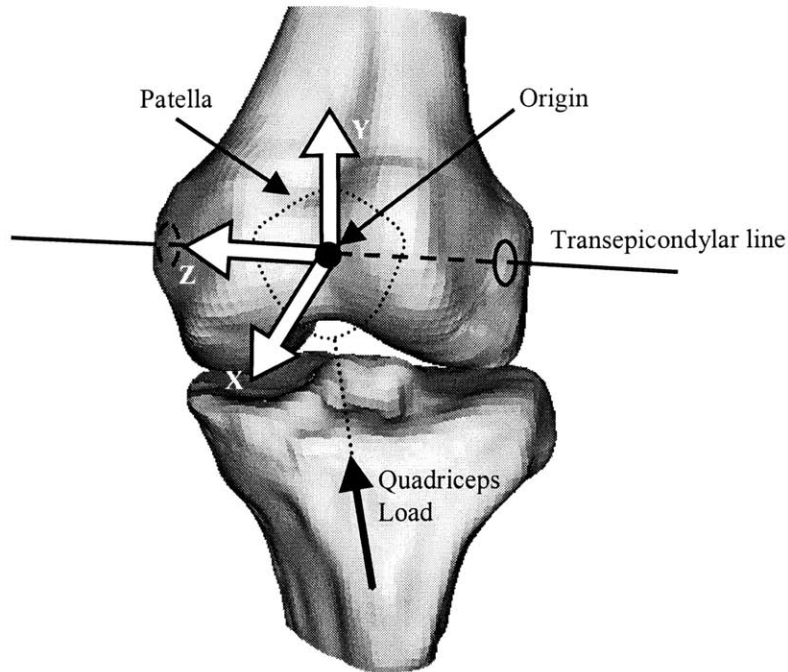


Figure 4. Initial position of the tibial and femoral coordinate systems (CS). The anterior-posterior tibial forces were applied to the tibia at the origin of the tibial CS along the x-axis. The quadriceps load was applied to the tibia along the patellar tendon, which connects the tibial tuberosity and the patellar tendon.

It was also necessary to define points of application for the forces applied to the knee in the following simulations. All the anterior-posterior tibial loads were applied at the origin of the tibial coordinate system (Figure 4). The application of the quadriceps load was chosen along the central line of the patellar tendon, which was determined from X-ray images of the knee in sagittal and coronal planes obtained during experiment. The orientation of the patellar tendon central line was determined at 0, 30, 60, and 90° of flexion.

2.1.3 Optimization

Certain parameters of the knee joint model, namely the zero-load lengths of the ligament bundles and the rigidity values of the meniscus elements, are not easily measured by experiment. Thus, a minimization procedure was used in order to determine the optimal values for these parameters [32, 85, 91]. The first step in the optimization process was to test the knee used to build the model using a robotic testing system [32, 77, 91]. Various external loads were applied to the knee while the knee kinematics and ligamentous tensions were measured. In this test, the knee was subjected to anterior-posterior (AP) tibial loads up to $\pm 134\text{N}$ (in increments of 26.8N) and internal-external (IE) tibial moments up to $\pm 10\text{Nm}$ (in increments of 2Nm). The robot measured the knee kinematics in 5 DOF with the flexion angle fixed at 0° , 30° , 60° , and 90° of flexion.

The anterior-posterior tibial load up to $\pm 134\text{ N}$ and the internal-external moment up to $\pm 10\text{Nm}$, as used in the intact knee test, were applied to the tibia of the model. The difference between tibial translations and rotations predicted by the model, t and r , and the translations and rotations measured by the robot, T and R , were minimized using the following objective function:

$$\min_{l_{o,i}, k_{m,j}} g = \left\{ \sum_{n=1}^{10} \left(\frac{|T-t|}{T} \right)^2 + \sum_{s=1}^{10} \left(\frac{|R-r|}{R} \right)^2 \right\}^{1/2} \quad (3)$$

where $l_{o,i}$ represents the zero-load length of each ligament element ($i = 1$ to 16) and $k_{m,j}$ represents the rigidity of each meniscus element ($j = 1$ to 6). The parameter n represents a summation over the ten AP tibial loads, and the parameter s represents a summation over the ten IE tibial moments. The zero-load lengths of the ligament bundles and menisci rigidities were adjusted until $g < 0.2$. The optimization was carried out at 0 , 30 , 60 , and 90° of flexion. The optimized slack lengths of the bundles are given in Table 2 along with the rigidities of the bundles.

Table 2. Axial Rigidities and Slack Lengths for Ligament Bundles and Meniscus Elements

Ligament/ Meniscus	Bundle/Element	Rigidity (N)	Slack (mm)
ACL	Anterior element of AM bundle	2500	0.0
	Posterior element of AM bundle	2500	0.1
	Anterior element of PL bundle	2500	0.25
	Posterior element of PL bundle	2500	-0.17
PCL	Anterior element of AL bundle	4500	9.0
	Posterior element of AL bundle	4500	6.0
	Anterior element of PM bundle	4500	9.0
	Posterior element of PM bundle	4500	5.2
LCL	Anterior bundle	2000	0.0
	Inferior bundle	2000	0.0
	Posterior bundle	2000	0.0
MCL	Anterior bundle	2750	4.8
	Inferior bundle	2750	1.3
	Posterior bundle	2750	0.0
	Anterior capsular fibers	1000	5.0
	Posterior capsular fibers	1000	0.0

AM = Anterior medial, PL = Posterior lateral

AL = Anterior lateral, PM = Posterior medial

After optimization the kinematics calculated by the computational model closely matched the experimental data of the native knee in both translation and rotation under the AP loads and IE moments at different flexion angles (Figure 5). At 0° of flexion, the anterior tibial translations calculated from the model and measured from the experiment were 4.5 mm and 3.9 mm, respectively, under the 134 N anterior tibial load and -6.2 mm and -6.5 mm, respectively, under the posterior tibial load (Figure 5a).

Under 10 Nm IE moments, the model calculated 22.6° of internal tibial rotation and -24.8° external tibial rotation at 90° of flexion. Under the same loading conditions, the experiment measured 21.9° of internal tibial rotation and -20.0° of external rotation (Fig. 5h). Similar comparisons between the computational model and experimental measurement were observed at both 30° and 60° of flexion of the knee.

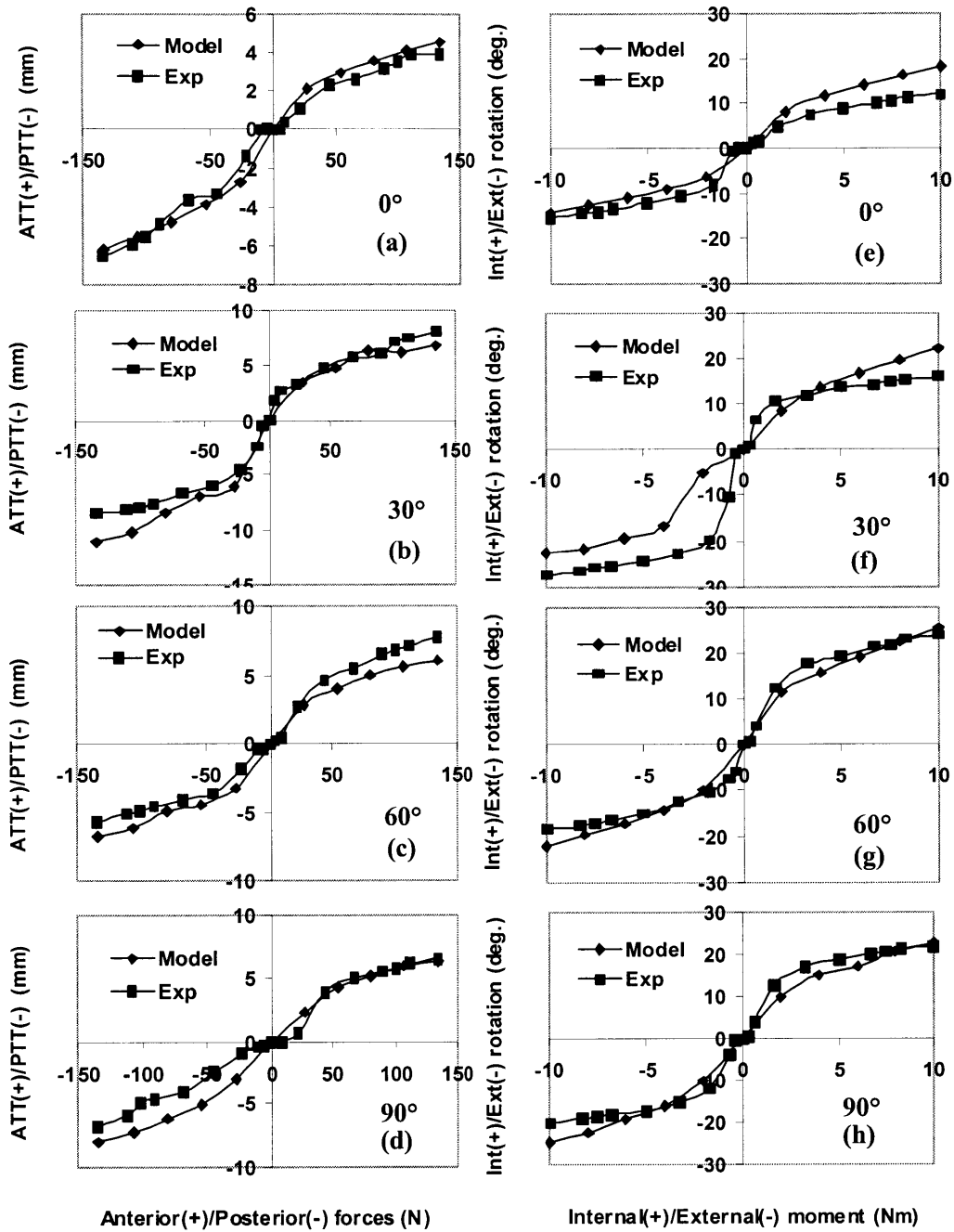


Figure 5. Comparison of knee kinematics predicted from the 3D knee model and measured from robotic experiment at different flexion angles. The graphs on the left represent the anterior-posterior tibial translation (ATT and PTT) under 134N AP load at **a)** 0°, **b)** 30°, **c)** 60°, and **d)** 90°. The graphs on the right represent the internal-external tibial rotation (Int and Ext) under 10 Nm int-ext moment at **e)** 0°, **f)** 30°, **g)** 60°, and **h)** 90°.

2.1.4 Validation

Validation of the knee model was carried out by comparing the kinematics and ligamentous tensions predicted using the model with those measured from experiments, where one experiment used 8 knee specimens [92] and another used 12 specimens [93].

The knee kinematics predicted by the model was compared with those measured from cadaveric human specimens (n=8) under a 400 N quadriceps load [92] (Figure 6). In general, the predicted anterior tibial translation was within the experimental data (Figure 6a). At full extension of the knee, the model predicted an anterior tibial translation of 3.8 mm, while the experiment measurement was 2.6 ± 1.0 mm. The model predicted a 5.0 mm anterior tibial translation at 30° of flexion, which corresponded with a 5.6 ± 1.2 mm translation measured from experiment. The model predicted internal tibial rotation of 4.6° and 6.8° at full extension and 30° of flexion, respectively (Figure 6b). At these two flexion angles, experimental measurements were $2.6 \pm 1.4^\circ$ and $6.9 \pm 1.4^\circ$, respectively.

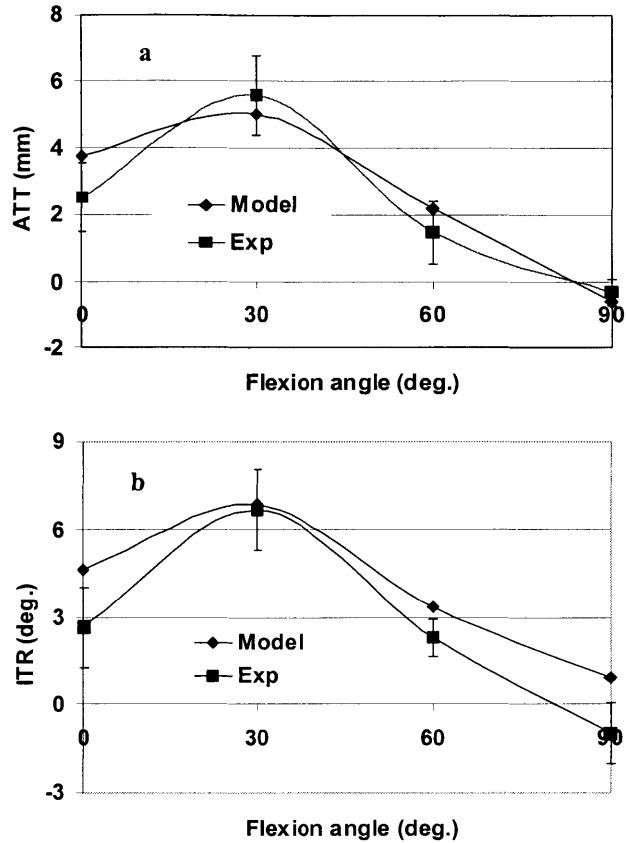


Figure 6. Comparison of **a)** anterior tibial translation (ATT) and **b)** internal tibial rotation (ITR) predicted from the 3D knee model and measured from in-vitro experiment at different flexion angles under a 400 N quadriceps load.

The model also predicted tibial rotation under a 10 Nm internal tibial torque that was within the range of experimental data measured from 12 specimens [93] (Figure 7). For example, at 30° of flexion, the model predicted a 22.3° internal tibial rotation. The experimental data showed a 20.5±2.1° internal tibial rotation under the same loading condition.

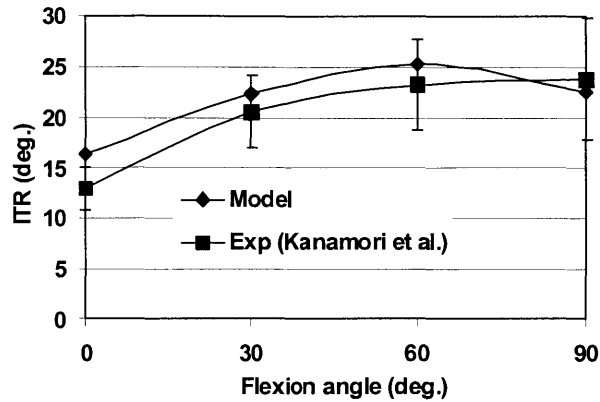


Figure 7. Comparison of internal tibial rotation (ITR) predicted from the 3D knee model and measured from in-vitro experiment at different flexion angles under a 10 Nm internal tibial moment.

Figure 8 shows the comparison of the forces in the ACL and the PCL calculated from the model with those of the experimental measurements conducted in our laboratory. Under a 400 N quadriceps load, the model predicted a 92.3 N ACL force at full extension, and the experiment measured 63.4 ± 33.4 N under the same loading condition (Figure 8a) [92]. At 30° of flexion, the model prediction and experimental measurement were 98.9 N and 71.7 ± 27.9 N, respectively. While under a 134 N posterior tibial load (Figure 8b), the forces in the PCL of 0 N and 21.0 ± 19.5 N were predicted by the model and measured from the experiment, respectively, at full extension. At 90° of flexion, the model predicted a PCL force of 115.8 N, while the experiment measured a 96.6 ± 18.2 N PCL force.

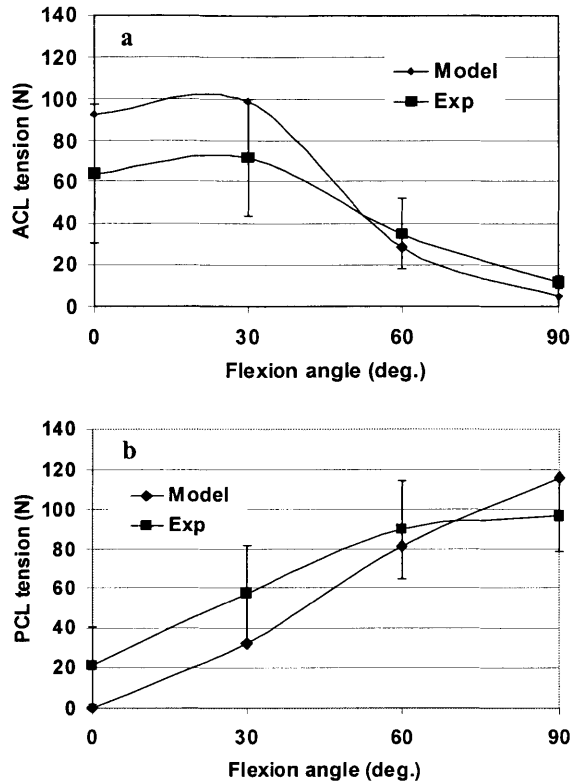


Figure 8. Comparison of a) ACL forces under a 400N quadriceps load and b) PCL forces under a posterior tibial load of 134N predicted from the 3D knee model and measured from in-vitro experiment at different flexion angles.

2.2 Simulations of ACL Injury and Reconstruction

This study uses a computational knee joint model constructed from MR images of a cadaveric knee. The contours of the tibia, femur, and articular cartilage were digitized from the MR images and used to create the model surfaces. Besides the bone and articular cartilage, the model also included multi-bundle representations of the ACL, PCL, LCL, and MCL along with a simplified representation of the menisci. The model was optimized by comparing model predictions to experimental data obtained from testing of the same knee used to construct the model. The model was then validated by comparing its predictions to experimental data obtained from knee specimens tested under various loading conditions.

2.2.1 ACL Injury Simulation

A simple modeling of injury to the ACL to varying degrees was performed by reducing the axial rigidity of the ACL elements. The axial rigidity of the ACL was reduced by 25, 50, 75, and 100%. Rigidity reduction of 25 to 75% represented partial injury, and reduction by 100% represented complete ACL rupture. A quadriceps load of 400N was applied in the knee model. The knee model was analyzed at four different flexion angles: 0°, 30°, 60°, and 90°. At each flexion angle, the femur was fixed, and the tibia was allowed to move in the other 5 degrees of freedom under external loads. Knee kinematics, including anterior-posterior tibial translation and internal-external tibial rotation, ligamentous tension, and peak contact pressure on the cartilage surface, were analyzed.

2.2.2 ACL Reconstruction Simulation

To simulate ACL reconstruction using single bundle grafts, the ACL in the model was replaced with a graft modeled with a single nonlinear spring element. Grafts with three different axial rigidities were used in this study. Graft 1 had a rigidity similar to the intact ACL, Graft 2 had a rigidity similar to that of a 10mm BPTB graft, and Graft 3 had a rigidity similar to that of a 14mm BPTB graft [2, 74, 94] (Table 3). The ACL deficient case was analyzed by using a graft with zero axial modulus. The initial graft tension was set to 0 N or 40 N with the knee at 30° of flexion [46, 47] by adjusting the zero load length of the graft. The graft tunnels were modeled according to the ACL reconstruction technique described by Clancy et al. [95] (Figure 9). The graft was assumed to be rigidly fixed to the bone at the mid-length of each tunnel. Contact between the graft and the tunnel was assumed to otherwise be frictionless.

Table 3. Axial Rigidity of the ACL and various Grafts (kN) adopted from literature.

Graft	Hamner ^{a,c} (1999)	Noyes ^{a,c} (1984)	Noyes ^{b,c} (1984)	Cooper ^{b,c} (1993)	Woo ^{b,d} (1991)	Butler ^{b,e} (1986)	Model
ACL	-	4.9	-	-	6.5	13.3	10
BPTB, 10mm	-	-	-	22.8	-	23	20
BPTB, 14mm	-	18.4	31.0	27.8	-	32.2	30
Semitendinosus	6.4	5.0	15.1	-	-	-	-
QST/G	23.3	-	-	-	-	-	-

^a Soft tissue was held directly by grips.

^b Soft tissue was left attached to bone or markers were used to measure local strain.

^c Hamner et al., Noyes et al. and Cooper et al. report structural stiffness based on lengths of 30, 26.9, and 50 mm, respectively.

^d Length measurements from Noyes et al. were used to convert reported structural stiffnesses to axial rigidity.

^e Area measurements from Noyes et al. were used to convert reported Young's Moduli to axial rigidity.

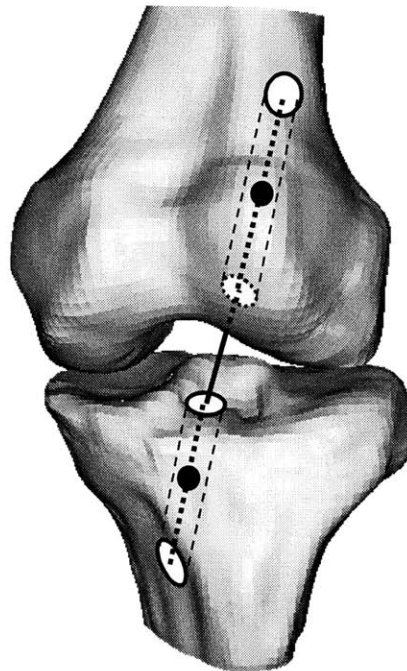


Figure 9. Graft is fixed to the bone halfway through the tunnels (denoted by black dots).

A simulated 134 N anterior drawer load was applied to the tibia while the knee was fixed at 0°, 30°, and 60°, and 90° of flexion [15, 71]. The anterior drawer load was applied at the knee center, which was defined as the midpoint of the transepicondylar line (Figure 4). The femur was held fixed in space while the tibia was allowed to move in all

degrees of freedom except flexion. The model was analyzed in intact ACL, ACL deficient (complete rupture), and ACL reconstructed states using the three grafts and two initial tensions described above. The calculated anterior tibial translation (ATT), internal tibial rotation (ITR), and ACL/graft tension were recorded. The process was repeated at all targeted flexion angles with a 400 N quadriceps load applied to the tibia instead of the anterior drawer load. The vector of the quadriceps force was determined by the orientation of the inferior pole of the patella with respect to the tibial tubercle using radiographs of the cadaver knee used to build the model (Figure 4). The patellofemoral joint was not included in the model.

3. Results

3.1 Stiffness Reduction

The anterior tibial translation (ATT) in the intact knee increased with increasing flexion from 0 to 30° of flexion under the quadriceps load. Maximal anterior tibial translation was observed at 30° of flexion, where the anterior tibial translation was 5 mm (Figure 10a). The ATT decreased with increasing flexion from 30 to 90° of flexion. ACL rupture (100% reduction of the ACL stiffness) caused increases of both ATT and internal tibial rotation (ITR) under the quadriceps muscle load at all selected flexion angles (Figure 10). At 30° of flexion, where the maximum ATT occurred, a 25% reduction in ACL stiffness produced only a 4% increase in ATT, and a 50% reduction in stiffness produced a 10% increase in ATT compared to the intact motion. While a reduction of 75% of the ACL stiffness resulted in a 20% increase in anterior tibial translation (Figure 10c), the rupture of the ACL caused a 44% increase under the same loading condition.

The ITR in the intact knee also increased with increasing flexion from 0 to 30° flexion with a maximum of 7° and then decreased with increasing flexion from 30 to 90° of flexion (Figure 10b). At 30° of flexion, a 25% reduction in the ACL stiffness produced a 4% increase in ITR, and a 50% stiffness reduction produced an 11% increase in ITR compared to the intact motion. A reduction of 75% of the ACL stiffness resulted in a 20% increase in ITR (Figure 10c). ITR was increased to 10.0°, a 48% increase, when the ACL was completely ruptured. .

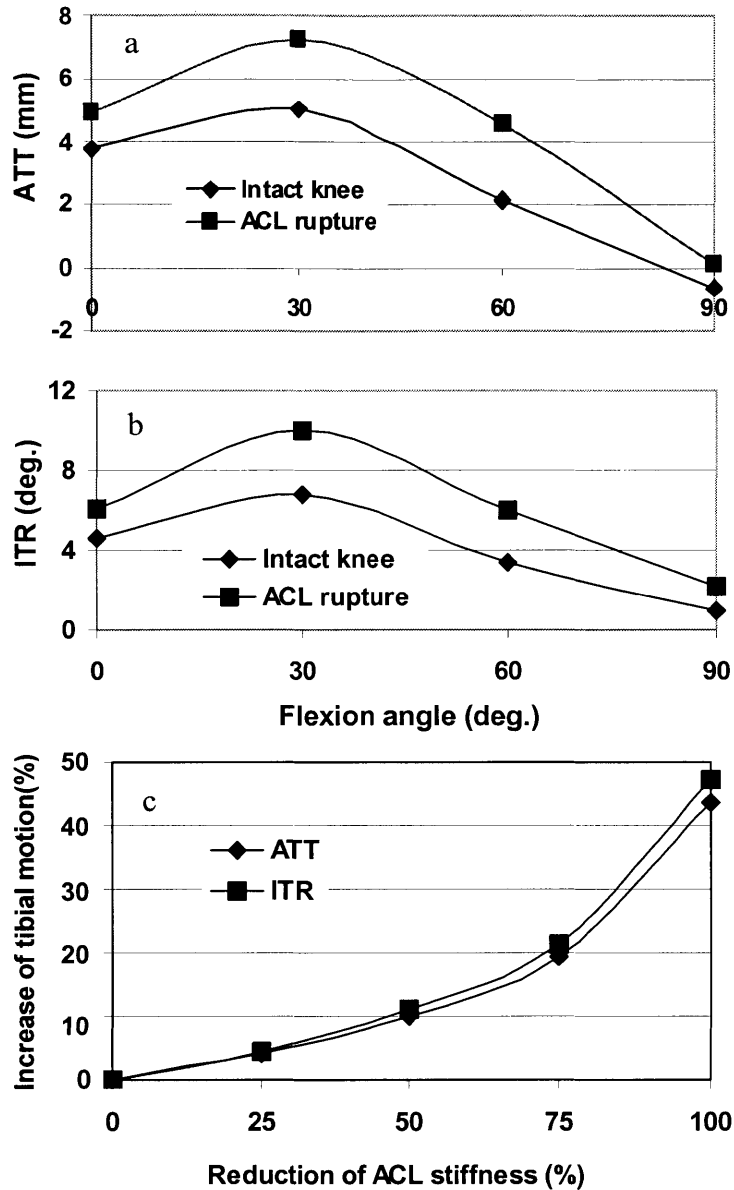


Figure 10. a) Anterior tibial translation (ATT) before and after simulated ACL rupture; b) internal tibial rotation (ITR) before and after simulated ACL rupture; and c) relative changes of anterior tibial translation and internal tibial rotation caused by reduction of ACL stiffness at 30° of flexion under the quadriceps muscle load.

The peak force in the intact ACL was 99 N under the 400 N quadriceps load at 30° of flexion (Figure 11a). The ACL force increased slightly from 0 to 30° of flexion and then decreased with increasing flexion from 30 to 90° of flexion. At 30° of flexion, a 25% reduction in the ACL stiffness reduced the ACL force by only 9%. With a 50% reduction in ACL stiffness, the force in the ACL graft was reduced to 78 N, a 20%

decrease in ACL force compared to the intact value. As the ACL stiffness was reduced by 75%, the ACL force was approximately 60 N, representing an approximate 40% decrease of intact ACL force. The contact pressure most affected by the state of the ACL was the lateral contact pressure at 30° of flexion. A 50% reduction in ACL stiffness increased this contact pressure by only 5% (Figure 11b). However, a 75% reduction in ACL stiffness increased the contact pressure by 18%, and complete rupture of the ACL increase the pressure by 41%

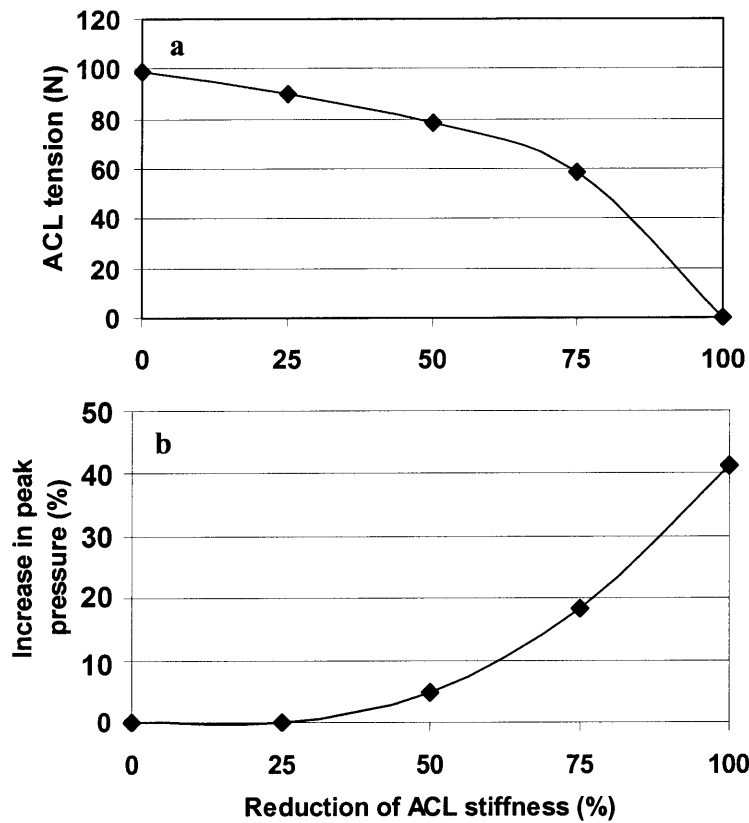


Figure 11. a) ACL forces and b) increases of peak lateral contact pressure caused by the reduction of ACL stiffness predicted at 30° of flexion using the computational model when subjected to the quadriceps muscle load.

3.2 Reconstruction

3.2.1 Anterior Tibial Drawer

Under the 134 N anterior drawer load, ATT in the intact knee increased with flexion from 0° to 30° of flexion with a peak ATT of 5.3 mm and then decreased slightly from 30° to 90° of flexion (Table 3). ATT of the ACL deficient knee followed the same

trend, but the magnitude was 30 to 40% greater than that of the intact knee. The peak ATT for the ACL deficient knee was 7.2 mm, which was 36% greater than the intact value. ITR of the knee in all states had local minimums at 0° and 60° of flexion and local maximums at 30° and 90° (Table 3). ITR of the deficient knee was 15 to 50% greater than that of the intact knee. The intact ACL tension increased slightly with increasing flexion from 0° to 30° peaking at 97 N and then gradually decreased from 30° to 90° of flexion (Table 3).

Table 4. Anterior tibial translation, internal tibial rotation and ACL/graft tension of the knee in intact, ACL deficient and ACL reconstructed conditions in response to a 134 N anterior tibial load. Two initial graft tensions (0 N and 40 N) were simulated.

Flexion Angle(°)		0 N Initial Tension			40 N Initial Tension			Deficient
Intact		Graft 1	Graft 2	Graft 3	Graft 1	Graft 2	Graft 3	
Anterior Tibial Translation (mm)								
0	3.5	3.8	3.5	3.2	2.8	2.5	2.3	4.7
30	5.3	5.7	5.1	4.8	4.3	3.9	3.6	7.2
60	5.0	5.4	4.9	4.5	4.1	3.7	3.5	7.0
90	4.9	5.3	4.9	4.7	4.2	3.9	3.8	6.4
Internal Tibial Rotation (°)								
0	3.6	4.0	3.6	3.3	2.9	2.5	2.2	5.1
30	5.2	5.7	5.0	4.5	3.9	3.3	3.0	7.9
60	3.2	3.3	3.1	3.1	3.0	2.8	2.7	3.7
90	5.6	5.9	5.5	5.3	4.7	4.5	4.3	7.4
ACL/Graft Tension (N)								
0	84.8	65.4	93.6	111.0	134.6	156.5	168.5	0.0
30	97.5	77.3	105.2	121.2	138.7	155.3	163.2	0.0
60	89.9	72.3	95.5	108.6	126.2	140.1	148.0	0.0
90	72.9	51.7	70.3	81.5	103.5	115.4	122.1	0.0

After ACL reconstruction, the ATT, ITR, and graft tension of the knee followed the same trends with respect to flexion angle as the intact knee under the anterior drawer load (Table 3). All ACL reconstructions reduced the ATT compared to the ACL deficient knee at all the selected flexion angles. When the initial graft tension was set to 0 N, ACL reconstruction using Graft 1 produced a peak ATT of 5.7 mm at 30° of flexion, which was 8% greater than that of the intact knee at the same flexion angle.

Reconstruction using Grafts 2 and 3 produced peak ATTs of 5.1 and 4.8 mm, respectively, at 30° of flexion. These translations were 3% and 10% less than the ATT of the intact knee, respectively. The ITR at 30° of flexion when using Graft 1 was 5.7°, 10% greater than the intact ITR (Table 3). The ITRs when using Grafts 2 and 3 were 5.0° and 4.5°, which were 4% and 13% less than the intact ITR, respectively. Peak graft tension was also observed at 30° of flexion in all three grafts. When Graft 1 was used, the peak tension was 77 N, which was 21% less than the intact ACL (Table 3). Graft 2 had a peak tension of 105 N, which was 8% greater than the intact ACL, and Graft 3 had a peak tension of 121 N, which was 24% greater than that of the intact ACL.

When the initial graft tension was set to 40 N, ACL reconstruction using Grafts 1, 2, and 3 produced peak ATTs of 4.3, 3.9, and 3.6 mm, respectively, at 30° of flexion under the anterior drawer load (Table 3). These ATTs were 18%, 27%, and 32% less than that of the intact knee. The ITRs at 30° of flexion for Grafts 1, 2, and 3 were 3.9°, 3.3°, and 2.9°, which were 24%, 36%, and 43% less than the intact ITR, respectively. The graft tensions at 30° of flexion were 139, 155, and 163 N, respectively. These were 42%, 59% and 67% greater than that of the intact ACL (Table 3).

3.2.2 *Quadriceps force*

Under the quadriceps load, ATT in the intact knee increased with increasing flexion peaking at 30° with an ATT of 4.9 mm (Table 4). The ATT then decreased as flexion increased from 30° to 90°. ATT in the ACL deficient knee followed the same trend as the intact knee with a 7.0 mm peak ATT, a 43% increase from the intact knee. ITR in the intact knee also increased with increasing flexion, peaking at 30°, and then decreased from 30° to 90° of flexion (Table 4). The ITR of the intact knee at 30° of flexion was 6.8°. In the ACL deficient knee, the ITR at 30° of flexion was 10.0°, 47% greater than the intact ITR. The absence of the ACL had very little effect on ATT and ITR at 90° of flexion. The intact ACL tension increased slightly from 0° to 30° of flexion, with a peak tension of 98 N (Table 4). Beyond 30° of flexion, the ACL tension dramatically decreased to 0 N at 90° of flexion. As was the case under the anterior tibial

drawer load, the most extreme behavior under the quadriceps load tended to occur at 30° of flexion.

Table 5. Anterior tibial translation, internal tibial rotation and ACL/graft tension of the knee in intact, ACL deficient and ACL reconstructed conditions in response to a 400 N quadriceps load. Two initial graft tensions (0 N and 40 N) were simulated.

Flexion Angle(°)	Intact	0 N Initial Tension			40 N Initial Tension			Deficient
		Graft 1	Graft 2	Graft 3	Graft 1	Graft 2	Graft 3	
Anterior Tibial Translation (mm)								
0	3.6	3.6	3.6	3.6	3.6	3.6	3.6	3.6
30	4.9	5.3	4.7	4.3	3.8	3.4	3.1	7.0
60	2.1	2.0	2.0	1.9	0.7	0.9	1.0	2.1
90	-2.5	-2.5	-2.5	-2.5	-2.5	-2.5	-2.5	-2.5
Internal Tibial Rotation (°)								
0	4.8	5.4	4.7	4.4	3.9	3.3	2.9	6.3
30	6.8	7.5	6.5	5.9	5.1	4.4	3.9	10.0
60	4.5	4.4	4.4	4.3	2.5	2.9	3.0	4.5
90	-4.3	-4.3	-4.3	-4.3	-4.3	-4.3	-4.4	-4.3
ACL/Graft Tension (N)								
0	92.4	70.0	102.1	122.4	144.6	168.7	181.2	0.0
30	97.7	77.7	103.7	117.7	132.6	144.7	150.0	0.0
60	0.0	1.4	2.4	3.0	19.9	18.4	18.1	0.0
90	0.0	0.0	0.0	0.0	0.0	0.0	0.0	0.0

After ACL reconstruction, the ATT, ITR, and graft tension of the simulated ACL reconstructions generally followed the trends of the intact knee under the quadriceps load (Table 4). With an initial graft tension of 0 N, ACL reconstruction using Graft 1 produced a peak ATT at 30° of flexion of 5.3 mm, which was 9% greater than that of the intact knee. When the knee was reconstructed using Grafts 2 and 3, the peak ATTs of 4.7 and 4.3 mm, respectively, also occurred at 30° of flexion. These values were 4% and 12% less than the intact knee, respectively. At 30° of flexion, the ITR of the knee reconstructed with Graft 1 was 7.5°, 10% greater than that of the intact knee. The ITRs when Grafts 2 and 3 were used were 6.5° and 5.9°, which were 4% and 13% less than the intact ITR, respectively. Graft 1 experienced a peak tension of 78 N, which was 20% less than the intact ACL tension, at 30° of flexion (Table 4). The tension in Graft 2 was 104

N, 6% greater than the intact ACL tension. The tension in Graft 3 was 118 N, which was 20% greater than the intact ACL tension.

When the ACL was reconstructed with a 40 N initial graft tension, the resulting ATT and ITR under the quadriceps load were less than those obtained when a 0 N initial graft tension was used (Table 4). Grafts 1, 2, and 3 produced ATTs of 3.8, 3.4, and 3.1 mm, respectively, at 30° of flexion. These translations were 22%, 31% and 36% less than that of the intact knee. The ITRs at 30° of flexion when Grafts 1, 2, and 3 were used were 5.1°, 4.4°, and 3.9°, which were 25%, 36%, and 43% less than the intact ITR, respectively. The tension of Graft 1 at 30° of flexion was 133 N, 36% greater than that of the intact ACL tension (Table 4). The tensions in Grafts 2 and 3 were 145 and 150 N, which were 48% and 53% greater than the intact ACL tension.

4. Discussion

Various factors may influence the biomechanical functions of the knee after ACL injury or reconstruction. Computational knee joint models, if validated appropriately, have the advantage of being useful for performing parametric studies for ACL injury or reconstruction. Constructing a knee model that can closely predict experimental data under various external loads and flexion angles has always been a challenge in computational biomechanics [32, 35, 82, 83, 85, 96, 97]. This work utilizes a computational knee joint model to conduct parametric analysis of ACL injury and reconstruction. This model was constructed using MR images and validated using experimental data of different specimens. In general, the kinematics and ligament forces predicted by the model were within the range of the experimental data measured from different specimens over a wide range of loading conditions and flexion angles. For example, under the quadriceps load, this model predicted that the anterior tibial translation increased from full extension to 30° of flexion and then decreased as flexion continued to increase. This result was consistent with those of Hirokawa et al [25] and Li et al. [29]. Therefore, the model can be used to conduct parameteric studies on knee joint biomechanics.

4.1 ACL Injury

The results of this computational model showed that the effect of reductions of ACL stiffness on knee joint function depends non-proportionally on the magnitude of the stiffness reduction of the ACL. With a 0 to 75% reduction of the intact ACL stiffness, the peak surface contact pressure was raised by less than 20%, while the ACL still carried more than 58% of the load carried by an intact ACL. When the ACL stiffness was reduced by more than 75% of the intact value, both contact pressure and ACL tension changed radically. With a complete rupture of the ACL (100% stiffness reduction), peak contact pressure was raised by more than 40%. Both anterior tibial translation and tibial rotation were also increased by more than 40%.

Partial ACL injury has been reported as ligament bundle damage in literature [98-100]. This paper simulated ACL injury simply by reducing the ACL stiffness in the model. Therefore, the results of this paper might not be able to accurately describe ligament bundle rupture. However, simulation of partial ACL injury can be improved by removing ligament elements of the ACL (e.g., anterior and medial elements for AM bundle, posterior and lateral elements for PL bundle) from the model. Another important factor in partial ACL injury is the changing of the reference length (zero-load length) of the ACL due to the injury. The change in reference lengths cannot be measured directly. A parametric study using the model, however, can provide useful information on the combined effect of the stiffness reduction and the reference length change of the ACL on knee biomechanics. This topic is currently under investigation.

Various animal studies have reported weakening of ACL grafts over time [101-105] It has been reported that the stiffness of ACL grafts was reduced by up to 60% of the control ACL values three years after surgery in an in-vivo goat model [101]. Beynnon et al showed the ACL graft stiffness was reduced up to 80% one year after operation in canine models [102]. In a rabbit model, Ballock et al demonstrated that the ACL graft stiffness was reduced by 76% fifty-two weeks after surgery [103]. It is difficult to measure the stiffness changes of ACL grafts in human subjects during healing. Beynnon et al reported knee laxity and material properties of a 10mm BPTB graft 8 months after surgery [106]. The stiffness and ultimate failure load of the graft approached that of the intact ACL, although the graft did experience some stretching. Our data showed that reduced stiffness of the ACL decreases the forces in the ligament, thus elevating knee laxity and peak contact pressures under the quadriceps load. However, even with a reduction of 75% of the stiffness, the ACL will still carry a significant amount of the load carried by an intact ACL as shown in Figure 11a. The kinematics variation will be less than 20% as demonstrated in Figure 10c. Therefore, if the knee kinematics is used as a guideline, the ligament grafts reported in literature may still have the capability to restore the majority of the native knee kinematics under the quadriceps load. Further investigation of the knee function under other loading conditions is necessary, and an in-vitro experiment should be developed to validate the conclusion of the model prediction.

4.2 ACL Reconstruction

ACL reconstruction has been shown to be effective in restoring anterior knee stability [21, 46, 47]. However, clinical studies with long-term follow-up have reported an increased incidence of complications after ACL reconstruction, such as early joint degeneration or patellofemoral joint pain, suggesting that ACL reconstruction may not be as efficient as expected in preventing long-term joint degeneration [4, 11, 18, 20, 21]. Current ACL grafts (BPTB, QST/G) have been shown to have axial moduli two to four times greater than that of the native ACL [2, 74, 75, 94] (Table 1). The supraphysiologic stiffness of the grafts may be a factor resulting in an over-constrained knee after ACL reconstruction. However, it is difficult to experimentally investigate the effect of variations in graft stiffness on knee kinematics.

The computer simulation demonstrated that the axial modulus of the graft has a considerable effect on kinematics of the ACL reconstructed knee. When the initial graft tension was set to 0 N, both Grafts 2 and 3 over-corrected the knee kinematics, and the graft tensions were higher than that of the intact ACL (Table 2). Only Graft 1, which had an axial modulus similar to the ACL, resulted in an under-corrected knee. When the initial graft tension was set to 40 N, all three grafts over-constrained the knee by more than 15%, and the corresponding graft tensions were more than 35% greater than the tension in the intact ACL. Comparing the results of these various ACL reconstructions, Graft 2 (which had an axial modulus two times that of the ACL) produced kinematics closest (2% over-constraint) to the intact knee when 0 N initial graft tension was used.

This simulation of ACL reconstruction fixed the graft at the mid-length of the tunnels making the actual graft length approximately twice that of the intact ACL. Thus, the linear structural stiffness (force per unit elongation of the whole structure) of Graft 1 was less than that of the ACL, even though its axial modulus was similar to the ACL. Consequently, Graft 1 offered less constraint to knee motion than the intact ACL. However, under a 40 N initial tension, the graft was pre-stretched through a significant portion of the toe region of the force-displacement curve [74, 85]. Thus, preloading the graft with this initial tension resulted in an over-constrained knee under the loading conditions used in this study. While Graft 2 had twice the axial modulus of the intact

ACL, its structural stiffness was actually similar to that of the native ACL since the graft was approximately twice as long as the ACL. Therefore, under 0 N initial graft tension, Graft 2 produced similar kinematics to the intact knee. However, preloading the graft with an initial tension of 40 N again over-constrained the knee kinematics under both loading conditions. The axial modulus of Graft 3 was such that its structural stiffness was greater than the intact ACL even though the graft was longer than the intact ACL. Consequently, the knee was over-constrained by this graft even under 0 N initial graft tension.

An over-constrained knee may be the result of a “tight” graft, meaning a graft with excessive structural stiffness or initial tension or an inappropriate combination of the two. The structural stiffness of the graft is not only dependent on the axial modulus of the graft, but also the graft length. In this study, Graft 2 had a structural stiffness similar to the intact ACL when the graft was fixed at the mid-length position of the tunnels even though its axial modulus was two times that of the ACL. However, if the graft were fixed at the articular inlet of the tunnels, the graft would have a greater structural stiffness than the ACL. Therefore, if the graft is fixed close to the articular inlets, a graft with axial modulus lower than a 10mm BPTB graft should be used. Conversely, if the graft were fixed at the outlet of the tunnels, the graft would have a structural stiffness less than the ACL. If this fixation is used, a graft with axial modulus greater than a 10mm BPTB graft should be used. Ishibashi et al [76] has observed the effect of tunnel fixation sites on anterior stability of the knee. Anterior knee laxity decreased as the fixation sites were moved closer to the articular openings of the tunnels. The distance between fixation sites may need to be adjusted depending on the graft material to assure the reconstruction has a structural stiffness similar to that of the intact ACL.

Over-constrained knee kinematics may result in increased joint contact forces. Decreased anterior tibial translation arising from over-constrained ACL reconstruction will reduce the moment arm of the patellar tendon. Under this condition, a greater quadriceps force will be required to produce the same extension moment as in the intact state. This increased quadriceps force results in increased patellar contact pressure [107, 108]. Similarly, decreased internal tibial rotation may also result in higher contact pressures in the lateral facet of the patellofemoral joint [109]. Therefore, restoration of

normal knee kinematics after ACL reconstruction may be necessary to protect the knee from over loading.

5. Advantages and Limitations of the Model

5.1 Advantages

Even though in-vivo strains of the ACL/graft during certain activities have been reported in literature [110], evaluation of in-vivo forces of ACL/graft as well as their effect on knee kinematics is still difficult to determine in human subjects. The most important factor that affects ACL/graft forces in living subjects is still unknown. Computational modeling, if validated appropriately, can provide a powerful alternative to predict the knee kinematics, ligamentous tension, and cartilage contact stresses when the knee is subject to various functional loads. The model is also able to simulate the effect of surgical parameters on knee kinematics. For example, initial tension of the ACL graft can be changed by varying the ligament zero-load lengths in the model. The insertion sites of the graft can also be changed to simulate the effect of graft orientation and location. ACL reconstruction using multi-bundle grafts can be simulated by increasing the number of nonlinear spring elements in the model. Further, in addition to anterior tibial and quadriceps loads, various physiological loading conditions, such as combined axial compression and muscle contraction during weight-bearing activities, can be conveniently simulated using the model. The model can be used indefinitely, and the results of a certain experiment on the model are not affected by previous experiments. An added benefit to computational modeling is the relatively low cost involved compared to experimental testing. We believe that 3D computational modeling will be a powerful tool in the investigation of the effect of various soft tissue injuries and surgical reconstructions on knee joint behavior.

5.2 Limitations

Despite the advantages of using 3D computational knee joint model, there are certain limitations in the current modeling method. It is noted that the model was validated under a 400 N quadriceps load, which is lower than the physiological loading magnitudes estimated for daily activities such as walking (may reach several times body weight). While higher loads could be applied to the model, the results of such simulations

would not be trustworthy because there is not sufficient evidence that the model can accurately predict knee behavior under such conditions. Current in-vitro experiments are also limited to low loading conditions. The model needs to be further validated under physiological loading levels in order to predict knee responses during daily activities. The magnitude of the loads applied in our experiments, especially the muscle loads, is limited primarily by the load capacity of certain components of our testing system. These components will need to be redesigned in order to attain greater testing loads.

Contact pressure of meniscus-cartilage interface was not included in this model due to the complexity that would be involved especially in determining the motion of the menisci. Since the menisci function to increase the contact area in the joint, the current model may underestimate the contact area and consequently overestimate the contact stresses of the cartilage, although the equivalent resistance of the menisci in anterior-posterior and medial-lateral directions was considered. The cartilage was modeled as a linearly elastic material, and the contact pressure represented the *effective* pressure of the solid and fluid phases of the cartilage. If fluid pressure and solid matrix stresses are of interest, the biphasic cartilage model [Mow, 1982 #1281; Wu, 1998 #1219] has to be used. The results presented in this work represent those of one knee specimen. To make the results statistically meaningful, more knee models will be constructed and validated. Each model will be constructed from the MR images and experimental data of its own natural knee specimen.

As in all other *in vitro* experiments, this model does not account for any changes that take place during the healing process. Therefore the data in this study can only relate to knee function immediately after reconstruction. As noted in Section 4.1, the material properties of the graft change with time [73, 101-106]. A study by Ishibashi et al has shown that the graft begins to adhere to the tunnel wall with time, which effectively changes the fixation point of the graft [111]. These changes in the graft could be addressed by estimating the changes in the properties for a given time period. The adjusted properties could then be used in the model to analyze knee behavior at that given time period after reconstruction. Another limitation having to do with fixation is the graft is assumed to be rigidly fixed to the bone. It has been shown that graft fixation may not be rigid [59, 69]. When this is the case, the structural stiffness of the overall ACL

reconstruction may be reduced. An elastic fixation element is currently being developed to simulate non-rigid fixation.

6. Conclusions and Future Work

6.1 Conclusions

In conclusion, computational modeling is a feasible, advantageous, and informative method for investigating knee joint function and factors affecting surgical treatment. In this work, a computational knee joint model was used to investigate the effect of ACL injury and variations in graft stiffness along with initial graft tension on kinematics of the knee. If the stiffness of the ACL decreased by 75%, the kinematics of the knee would not change more than 20%. Thus, partially injured ACL's may be able to provide the majority of stability provided by an intact ACL.

ACL reconstructions were simulated using grafts with axial moduli similar to the ACL, a 10mm BPTB graft, and a 14mm BPTB graft, under initial tensions of 0 N or 40 N. The graft with *structural stiffness* similar to that of the intact ACL best restored intact knee kinematics when it was placed anatomically and fixed with 0 N initial tension at 30° of flexion. All three grafts over-constrained the knee when fixed with a 40 N initial graft tension. Over-constraint of the knee should be avoided, but the abnormal forces induced by over-constraint may aid in the early development of degenerative changes. The structural stiffness of a graft, along with the initial graft tension, plays an important role in determining the outcome of ACL reconstruction. The structural stiffness depends on the axial modulus of the graft and the graft length, which is determined by the choice of fixation points. Therefore, a combination of axial modulus and fixation points should be chosen such that the structural stiffness of the ACL reconstruction is similar to that of the intact ACL.

6.2 Future work

The next major step in this work is to create more knee models in order to build some statistical significance to any conclusions drawn from their use. The model of ACL injury will be improved by sequentially removing ACL bundles in order to better represent injury to the ligament. The model of ACL reconstruction will be improved by developing a method to capture non-rigid fixation of the graft in the tunnels. Our recent

work showed that the zero-load length of the graft significantly affects the structural stiffness of the graft and can be manipulated by adjusting the fixation locations. The fixation location of the grafts within the tunnels of the model will be varied in order to determine guidelines for the optimal graft fixation points. A computational study of PCL reconstruction will also be carried out.

The overriding goal of this work is to gain more insight into the effect of various factors on joint degeneration. With that in mind, future studies will include more extensive use of the models in analyzing the stress distribution in the articular cartilage. In a previous study, Li et al determined the effect of variations in modeling of the cartilage on the peak stresses within the cartilage [112]. Five independent investigators constructed a model from the same set of MR images, the cartilage thickness of all the models was found to be within 8% of the average thickness at all sites. Changes of $\pm 10\%$ in the cartilage thickness were found to affect the predicted cartilage stresses by less than 10%. This leads to the conclusion that this modeling technique is a feasible tool for analyzing cartilage stress. As mentioned previously, cartilage degeneration is often seen in the patellofemoral joint, which is currently not included in the model [20]. However, relatively simple modifications could be made to include the interaction of the patellofemoral joint. Results obtained from the use of this model could provide valuable information on the cause of joint degeneration.

Appendix A: Cartilage Contact Algorithm

Modeling contact between surfaces can become a complex issue. In order to be useful, contact in the model had to be represented in simple yet reasonable manner. Thus, several assumptions were made regarding contact between the cartilage layers. Since the femur is fixed in space, only the equilibrium of the tibia is of concern, so the following derivation of the contact algorithm focuses on the deformation and force in the tibial cartilage.

A.1 Determination of Contact

The determination of contact between cartilage layers was achieved through a comparison of surface normals. Each cartilage surface element had a node in the center of the element. For each tibial node, a check was carried out with every femoral node to determine if there was contact. The process went as follows:

1. For a particular tibial node T and a particular femoral node F, the vector from T to F was calculated (ft) (Figure A.1). If the magnitude of ft (d_{ftji}) was larger than a preset value $d_{ft} = 2.0$ mm, it was assumed that nodes F and T were not in contact.

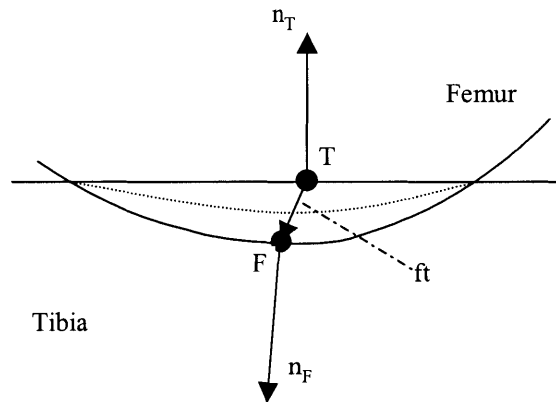


Figure A.1. Determination of contact by comparison of the vector from the tibial node to the femoral node and the femoral surface normal

2. If $d_{ftji} < d_{ft}$, d_{ft} was set equal to d_{ftji} , and the dot product of ft and the femoral surface normal, n_F , was calculated. ($aa = ft \cdot n_F$)

3. If $aa > 0.3$, vectors f_t and n_F were heading in somewhat the same direction, so F must have passed through the tibial surface. Nodes T and F were said to be in contact, and the femoral node number was recorded. ($j_{\text{contact}} = F$)
4. Repeat steps 1-3 for all femoral nodes with d_{ftji} equal to d_{ft} .
5. Repeat steps 1-4 for all tibial nodes.

A.2. Contact Force

The contact force, F_c , consists of a normal force F_n , which acts parallel to the surface normal n_t , and a shear force F_s , which act perpendicular to n_t (Figure A.2). A force F_t will be generated in the cartilage that is equal and opposite the contact force. The coefficient of friction between cartilage layers is very low, so friction between the layers was ignored. So we can write:

$$F_s = 0 \quad \Rightarrow \quad F_c = F_n = -F_t \quad (\text{A.1})$$

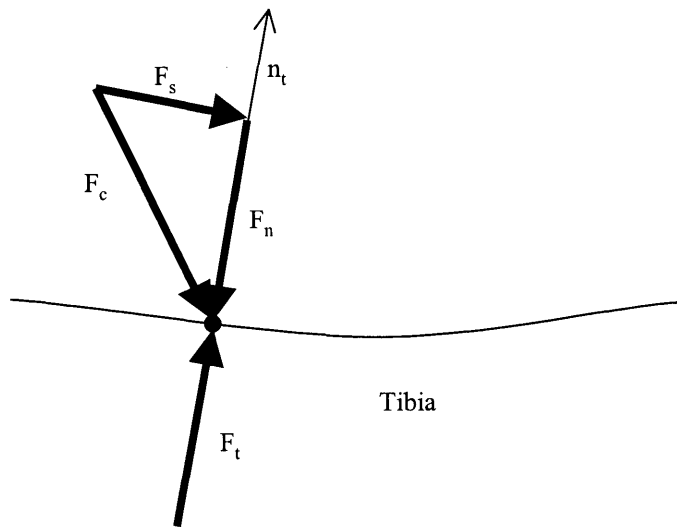


Figure A.2. Contact force on the tibial surface.

In reality, the surface normals of the tibia and femur at a point of contact will be parallel. However, since the geometry of the model was not modified throughout the simulations, the surface normals in the model were not necessarily parallel, and thus, the

forces generated in the cartilage, F_t and F_f , would not necessarily be parallel. For simplicity, this algorithm assumed the forces F_t and F_f were parallel with the tibial surface normal n_t . Given the facts that contact between blunt objects tends to flatten the contact surfaces and the tibia surface is more flat than the femoral surface, this is not a bad assumption.

A.3 Cartilage modeled as springs

Each cartilage surface node was at the head of spring, which ran in along the surface normal to the bone. The node was assumed to only move along the direction of the spring. For small deformations, the springs were assumed to be linear, so the forces in the tibial and femoral cartilage at a given point of contact were given by:

$$F_t = d_t k_t, \quad F_f = d_f k_f \quad (\text{A.2})$$

where d_t and d_f are the tibial and femoral spring deformations, and k_t and k_f are the tibial and femoral spring stiffnesses, respectively. The cartilage spring stiffness is given by [84]:

$$k = \frac{SA}{b} \quad (\text{A.3})$$

where S is the confined compression modulus, A is the surface area of the element, and b is the cartilage thickness at that point.

For large deformations, the force in the spring was given by:

$$F = SA \ln\left(1 - \frac{d}{b}\right) \quad (\text{A.4})$$

A.4 Cartilage deformation

Both layers of cartilage were assumed to deform. It is not possible to solve the large deformation formula (Equation A.4) for the deformations, so in determining the cartilage deformations, small deformations were assumed. After the deformations were determined, the calculated deformations were then substituted into either the small or large deformation formulas. The sum of the tibial and femoral deformation was assumed to be equal to the distance between the tibial and femoral nodes said to be in contact.

$$d_t + d_f = d_{tji} \quad (\text{A.5})$$

Using equations A.2 and A.5 and the fact that F_t and F_f must be equal in magnitude and assuming small deformations, we can write:

$$d_t k_t = d_f k_f = (d_{-ftji} - d_t) k_f \quad \Rightarrow \quad d_t = \frac{(d_{-ftji}) k_f}{k_t + k_f} \quad (\text{A.6})$$

References

1. Woo, S.L., J.M. Hollis, D.J. Adams, R.M. Lyon, and S. Takai, *Tensile properties of the human femur-anterior cruciate ligament-tibia complex. The effects of specimen age and orientation*. Am J Sports Med, 1991. **19**(3): p. 217-25.
2. Noyes, F.R., D.L. Butler, E.S. Grood, R.F. Zernicke, and M.S. Hefzy, *Biomechanical analysis of human ligament grafts used in knee-ligament repairs and reconstructions*. J Bone Joint Surg Am, 1984. **66**(3): p. 344-52.
3. Feagin, J.A., Jr., K.L. Lambert, R.R. Cunningham, L.M. Anderson, J. Riegel, P.H. King, and L. VanGenderen, *Consideration of the anterior cruciate ligament injury in skiing*. Clin Orthop, 1987(216): p. 13-8.
4. Daniel, D.M., M.L. Stone, B.E. Dobson, D.C. Fithian, D.J. Rossman, and K.R. Kaufman, *Fate of the ACL-injured patient. A prospective outcome study*. Am J Sports Med, 1994. **22**(5): p. 632-44.
5. Miyasaka, K.C., D.M. Daniel, and M.L. Stone, *The incidence of knee ligament injuries in the general population*. Am J Knee Surg, 1991. **4**: p. 3-8.
6. Belmont, P.J., Jr., S.B. Shawen, K.T. Mason, and S.J. Sladicka, *Incidence and outcomes of anterior cruciate ligament reconstruction among U.S. Army aviators*. Aviat Space Environ Med, 1999. **70**(4): p. 316-20.
7. Murrell, G.A., S. Maddali, L. Horovitz, S.P. Oakley, and R.F. Warren, *The effects of time course after anterior cruciate ligament injury in correlation with meniscal and cartilage loss*. Am J Sports Med, 2001. **29**(1): p. 9-14.
8. Frank, C.B. and D.W. Jackson, *The science of reconstruction of the anterior cruciate ligament*. J Bone Joint Surg Am, 1997. **79**(10): p. 1556-76.
9. Ferretti, A., F. Conteduca, A. De Carli, M. Fontana, and P.P. Mariani, *Osteoarthritis of the knee after ACL reconstruction*. Int Orthop, 1991. **15**(4): p. 367-71.
10. Hawkins, R.J., G.W. Misamore, and T.R. Merritt, *Followup of the acute nonoperated isolated anterior cruciate ligament tear*. Am J Sports Med, 1986. **14**(3): p. 205-10.
11. Dye, S.F., E.M. Wojtys, F.H. Fu, D.C. Fithian, and I. Gillquist, *Factors contributing to function of the knee joint after injury or reconstruction of the anterior cruciate ligament*. Instr Course Lect, 1999. **48**: p. 185-98.
12. L'Insalata, J.C., F.H. Fu, P.T. Irrgang, and C.D. Harner. *The International Knee Documentation Committee evaluation form form for assessment of outcome following anterior cruciate ligament reconstruction*. in *7th Congress of the European Society of Sports Traumatology, Knee Surgery and Arthroscopy, Budapest, Hungary*. 1996.
13. Plancher, K.D., J.R. Steadman, K.K. Briggs, and K.S. Hutton, *Reconstruction of the anterior cruciate ligament in patients who are at least forty years old. A long-term follow-up and outcome study*. J Bone Joint Surg Am, 1998. **80**(2): p. 184-97.
14. Grontvedt, T., L. Engebretsen, P. Benum, O. Fasting, A. Molster, and T. Strand, *A prospective, randomized study of three operations for acute rupture of the anterior cruciate ligament. Five-year follow-up of one hundred and thirty-one patients*. J Bone Joint Surg Am, 1996. **78**(2): p. 159-68.

15. Aglietti, P., G. Zaccherotti, R. Buzzi, and P. De Biase, *A comparison between patellar tendon and doubled semitendinosus/gracilis tendon for anterior cruciate ligament reconstruction. A minimum five-year follow-up.* J Sports Traumatol rel res, 1997. **19**(2): p. 57-68.
16. Deehan, D.J., L.J. Salmon, V.J. Webb, A. Davies, and L.A. Pinczewski, *Endoscopic reconstruction of the anterior cruciate ligament with an ipsilateral patellar tendon autograft. A prospective longitudinal five-year study.* J Bone Joint Surg Br, 2000. **82**(7): p. 984-91.
17. Aglietti, P., R. Buzzi, S. D'Andria, and G. Zaccherotti, *Long-term study of anterior cruciate ligament reconstruction for chronic instability using the central one-third patellar tendon and a lateral extraarticular tenodesis.* Am J Sports Med, 1992. **20**(1): p. 38-45.
18. Jomha, N.M., D.C. Borton, A.J. Clingeleffer, and L.A. Pinczewski, *Long-term osteoarthritic changes in anterior cruciate ligament reconstructed knees.* Clin Orthop, 1999(358): p. 188-93.
19. Shelbourne, K.D. and T. Gray, *Results of anterior cruciate ligament reconstruction based on meniscus and articular cartilage status at the time of surgery. Five- to fifteen-year evaluations.* Am J Sports Med, 2000. **28**(4): p. 446-52.
20. Jarvela, T., T. Paakkala, P. Kannus, and M. Jarvinen, *The incidence of patellofemoral osteoarthritis and associated findings 7 years after anterior cruciate ligament reconstruction with a bone-patellar tendon-bone autograft.* Am J Sports Med, 2001. **29**(1): p. 18-24.
21. O'Neill, D.B., *Arthroscopically assisted reconstruction of the anterior cruciate ligament. A follow-up report.* J Bone Joint Surg Am, 2001. **83-A**(9): p. 1329-32.
22. Buckwalter, J.A. and N.E. Lane, *Athletics and osteoarthritis.* Am J Sports Med, 1997. **25**(6): p. 873-81.
23. Fukubayashi, T., P.A. Torzilli, M.F. Sherman, and R.F. Warren, *An in vitro biomechanical evaluation of anterior-posterior motion of the knee. Tibial displacement, rotation, and torque.* J Bone Joint Surg Am, 1982. **64**(2): p. 258-64.
24. Woo, S.L., R.J. Fox, M. Sakane, G.A. Livesay, T.W. Rudy, and F.H. Fu, *Biomechanics of the ACL: Measurements of in situ force in the ACL and knee kinematics.* Knee, 1998. **5**(4): p. 267-288.
25. Hirokawa, S., M. Solomonow, Y. Lu, Z.P. Lou, and R. D'Ambrosia, *Anterior-posterior and rotational displacement of the tibia elicited by quadriceps contraction.* Am J Sports Med, 1992. **20**(3): p. 299-306.
26. Todo, S., Y. Kadoya, T. Moilanen, A. Kobayashi, Y. Yamano, H. Iwaki, and M.A. Freeman, *Anteroposterior and rotational movement of femur during knee flexion.* Clin Orthop, 1999(362): p. 162-70.
27. Daniel, D.M., L.L. Malcom, G. Losse, M.L. Stone, R. Sachs, and R. Burks, *Instrumented measurement of anterior laxity of the knee.* J Bone Joint Surg Am, 1985. **67**(5): p. 720-6.
28. Butler, D.L., F.R. Noyes, and E.S. Grood, *Ligamentous restraints to anterior-posterior drawer in the human knee. A biomechanical study.* J Bone Joint Surg Am, 1980. **62**(2): p. 259-70.

29. Li, G., T.W. Rudy, M. Sakane, A. Kanamori, C.B. Ma, and S.L. Woo, *The importance of quadriceps and hamstring muscle loading on knee kinematics and in-situ forces in the ACL*. J Biomech, 1999. **32**(4): p. 395-400.
30. Li, G., T.W. Rudy, C. Allen, M. Sakane, and S.L. Woo, *Effect of combined axial compressive and anterior tibial loads on in situ forces in the anterior cruciate ligament: a porcine study*. J Orthop Res, 1998. **16**(1): p. 122-7.
31. Li, G., K.R. Kaufman, E.Y. Chao, and H.E. Rubash, *Prediction of antagonistic muscle forces using inverse dynamic optimization during flexion/extension of the knee*. J Biomech Eng, 1999. **121**(3): p. 316-22.
32. Li, G., J. Gil, A. Kanamori, and S.L. Woo, *A validated three-dimensional computational model of a human knee joint*. J Biomech Eng, 1999. **121**(6): p. 657-62.
33. More, R.C., B.T. Karras, R. Neiman, D. Fritschy, S.L. Woo, and D.M. Daniel, *Hamstrings--an anterior cruciate ligament protagonist. An in vitro study*. Am J Sports Med, 1993. **21**(2): p. 231-7.
34. Torzilli, P.A., X. Deng, and R.F. Warren, *The effect of joint-compressive load and quadriceps muscle force on knee motion in the intact and anterior cruciate ligament-sectioned knee*. Am J Sports Med, 1994. **22**(1): p. 105-12.
35. Andriacchi, T.P., R.P. Mikosz, S.J. Hampton, and J.O. Galante, *Model studies of the stiffness characteristics of the human knee joint*. J Biomech, 1983. **16**(1): p. 23-9.
36. Andriacchi, T.P., C. Dyrby, and M. Dillingham. *ACL Injury Causes Rotational Abnormalities at the Knee During Walking*. in *Trans. Orthop. Res. Soc.* 2002. Dallas, TX: The Orthopaedic Research Society.
37. Tashman, S., W. Anderst, D. Collon, K. Anderson, and P. Kolowich. *Abnormal Tibio-Femoral Rotations During Stressful Activities after ACL Reconstruction*. in *Trans. Orthop. Res. Soc.* 2002. Dallas, TX: Orthopaedic Research Society.
38. Tashman, S. and W. Anderst, *In Vivo Knee Kinematics after ACL Reconstruction via High Speed Biplane Radiography*. Proceedings, 2nd International Symposium on Ligaments and Tendons, S. Woo et al., eds., Musculoskeletal Research Center, Dept. of Orthopaedic Surgery, UPMC Health System, Pittsburgh, PA, 2001. **2**: p. 8.
39. Markolf, K.L., A. Kochan, and H.C. Amstutz, *Measurement of knee stiffness and laxity in patients with documented absence of the anterior cruciate ligament*. J Bone Joint Surg Am, 1984. **66**(2): p. 242-52.
40. Markolf, K.L., A. Graff-Radford, and H.C. Amstutz, *In vivo knee stability. A quantitative assessment using an instrumented clinical testing apparatus*. J Bone Joint Surg Am, 1978. **60**(5): p. 664-74.
41. Seedhom, B.B., *Reconstruction of the anterior cruciate ligament*. Proc Inst Mech Eng [H], 1992. **206**(1): p. 15-27.
42. Takeda, Y., J.W. Xerogeanes, G.A. Livesay, F.H. Fu, and S.L. Woo, *Biomechanical function of the human anterior cruciate ligament*. Arthroscopy, 1994. **10**(2): p. 140-7.
43. Kanamori, A., J. Zeminski, T.W. Rudy, G. Li, F.H. Fu, and S.L. Woo, *The effect of axial tibial torque on the function of the anterior cruciate ligament: a*

- biomechanical study of a simulated pivot shift test. Arthroscopy*, 2002. **18**(4): p. 394-8.
44. Andriacchi, T.P., E.J. Alexander, M.K. Toney, C. Dyrby, and J. Sum, *A point cluster method for in vivo motion analysis: applied to a study of knee kinematics. J Biomech Eng*, 1998. **120**(6): p. 743-9.
 45. Takai, S., S.L. Woo, G.A. Livesay, D.J. Adams, and F.H. Fu, *Determination of the in situ loads on the human anterior cruciate ligament. J Orthop Res*, 1993. **11**(5): p. 686-95.
 46. Marder, R.A., J.R. Raskind, and M. Carroll, *Prospective evaluation of arthroscopically assisted anterior cruciate ligament reconstruction. Patellar tendon versus semitendinosus and gracilis tendons. Am J Sports Med*, 1991. **19**(5): p. 478-84.
 47. Aglietti, P., R. Buzzi, G. Zaccherotti, and P. De Biase, *Patellar tendon versus doubled semitendinosus and gracilis tendons for anterior cruciate ligament reconstruction. Am J Sports Med*, 1994. **22**(2): p. 211-7; discussion 217-8.
 48. Eriksson, K., P. Anderberg, P. Hamberg, A.C. Lofgren, M. Bredenberg, I. Westman, and T. Wredmark, *A comparison of quadruple semitendinosus and patellar tendon grafts in reconstruction of the anterior cruciate ligament. J Bone Joint Surg Br*, 2001. **83**(3): p. 348-54.
 49. Otero, A.L. and L. Hutcheson, *A comparison of the doubled semitendinosus/gracilis and central third of the patellar tendon autografts in arthroscopic anterior cruciate ligament reconstruction. Arthroscopy*, 1993. **9**(2): p. 143-8.
 50. Brand, J.C., Jr., D. Pienkowski, E. Steenlage, D. Hamilton, D.L. Johnson, and D.N. Caborn, *Interference screw fixation strength of a quadrupled hamstring tendon graft is directly related to bone mineral density and insertion torque. Am J Sports Med*, 2000. **28**(5): p. 705-10.
 51. Brown, C.H., Jr., A.T. Hecker, J.A. Hipp, E.R. Myers, and W.C. Hayes, *The biomechanics of interference screw fixation of patellar tendon anterior cruciate ligament grafts. Am J Sports Med*, 1993. **21**(6): p. 880-6.
 52. Burks, R.T. and R. Leland, *Determination of graft tension before fixation in anterior cruciate ligament reconstruction. Arthroscopy*, 1988. **4**(4): p. 260-6.
 53. Butler, D.L., Y. Guan, M.D. Kay, J.F. Cummings, S.M. Feder, and M.S. Levy, *Location-dependent variations in the material properties of the anterior cruciate ligament. J Biomech*, 1992. **25**(5): p. 511-8.
 54. Cooper, D.E., X.H. Deng, A.L. Burstein, and R.F. Warren, *The strength of the central third patellar tendon graft. A biomechanical study. Am J Sports Med*, 1993. **21**(6): p. 818-23; discussion 823-4.
 55. Fleming, B., B. Beynnon, J. Howe, W. McLeod, and M. Pope, *Effect of tension and placement of a prosthetic anterior cruciate ligament on the anteroposterior laxity of the knee. J Orthop Res*, 1992. **10**(2): p. 177-86.
 56. Fleming, B., B.D. Beynnon, R.J. Johnson, W.D. McLeod, and M.H. Pope, *Isometric versus tension measurements. A comparison for the reconstruction of the anterior cruciate ligament. Am J Sports Med*, 1993. **21**(1): p. 82-8.

57. Hoher, J., A. Kanamori, J. Zeminski, F.H. Fu, and S.L. Woo, *The position of the tibia during graft fixation affects knee kinematics and graft forces for anterior cruciate ligament reconstruction*. Am J Sports Med, 2001. **29**(6): p. 771-6.
58. Hoogland, T. and B. Hillen, *Intra-articular reconstruction of the anterior cruciate ligament. An experimental study of length changes in different ligament reconstructions*. Clin Orthop, 1984(185): p. 197-202.
59. Kurosaka, M., S. Yoshiya, and J.T. Andrish, *A biomechanical comparison of different surgical techniques of graft fixation in anterior cruciate ligament reconstruction*. Am J Sports Med, 1987. **15**(3): p. 225-9.
60. Lewis, J.L., W.D. Lew, L. Engebretsen, R.E. Hunter, and C. Kowalczyk, *Factors affecting graft force in surgical reconstruction of the anterior cruciate ligament*. J Orthop Res, 1990. **8**(4): p. 514-21.
61. Markolf, K.L., D.M. Burchfield, M.M. Shapiro, C.W. Cha, G.A. Finerman, and J.L. Slauterbeck, *Biomechanical consequences of replacement of the anterior cruciate ligament with a patellar ligament allograft. Part II: forces in the graft compared with forces in the intact ligament*. J Bone Joint Surg Am, 1996. **78**(11): p. 1728-34.
62. Markolf, K.L., D.M. Burchfield, M.M. Shapiro, B.R. Davis, G.A. Finerman, and J.L. Slauterbeck, *Biomechanical consequences of replacement of the anterior cruciate ligament with a patellar ligament allograft. Part I: insertion of the graft and anterior-posterior testing*. J Bone Joint Surg Am, 1996. **78**(11): p. 1720-7.
63. Markolf, K.L., J.F. Gorek, J.M. Kabo, and M.S. Shapiro, *Direct measurement of resultant forces in the anterior cruciate ligament. An in vitro study performed with a new experimental technique*. J Bone Joint Surg Am, 1990. **72**(4): p. 557-67.
64. Melby, A., 3rd, J.S. Noble, M.J. Askew, A.A. Boom, and F.W. Hurst, *The effects of graft tensioning on the laxity and kinematics of the anterior cruciate ligament reconstructed knee*. Arthroscopy, 1991. **7**(3): p. 257-66.
65. More, R.C. and K.L. Markolf, *Measurement of stability of the knee and ligament force after implantation of a synthetic anterior cruciate ligament. In vitro measurement*. J Bone Joint Surg Am, 1988. **70**(7): p. 1020-31.
66. Muneta, T., H. Yamamoto, H. Sakai, T. Ishibashi, and K. Furuya, *Relationship between changes in length and force in in vitro reconstructed anterior cruciate ligament*. Am J Sports Med, 1993. **21**(2): p. 299-304.
67. Paulos, L.E., D.L. Butler, F.R. Noyes, and E.S. Grood, *Intra-articular cruciate reconstruction. II: Replacement with vascularized patellar tendon*. Clin Orthop, 1983(172): p. 78-84.
68. Penner, D.A., D.M. Daniel, P. Wood, and D. Mishra, *An in vitro study of anterior cruciate ligament graft placement and isometry*. Am J Sports Med, 1988. **16**(3): p. 238-43.
69. Rowden, N.J., D. Sher, G.J. Rogers, and K. Schindhelm, *Anterior cruciate ligament graft fixation. Initial comparison of patellar tendon and semitendinosus autografts in young fresh cadavers*. Am J Sports Med, 1997. **25**(4): p. 472-8.
70. Stadelmaier, D.M., W.R. Lowe, O.A. Ilahi, P.C. Noble, and H.W. Kohl, 3rd, *Cyclic pull-out strength of hamstring tendon graft fixation with soft tissue*

- interference screws. Influence of screw length.* Am J Sports Med, 1999. **27**(6): p. 778-83.
71. Yasuda, K., J. Tsujino, Y. Tanabe, and K. Kaneda, *Effects of initial graft tension on clinical outcome after anterior cruciate ligament reconstruction. Autogenous doubled hamstring tendons connected in series with polyester tapes.* Am J Sports Med, 1997. **25**(1): p. 99-106.
 72. Bylski-Austrow, D.I., E.S. Grood, M.S. Hefzy, J.P. Holden, and D.L. Butler, *Anterior cruciate ligament replacements: a mechanical study of femoral attachment location, flexion angle at tensioning, and initial tension.* J Orthop Res, 1990. **8**(4): p. 522-31.
 73. Beynon, B.D., B.S. Uh, R.J. Johnson, B.C. Fleming, P.A. Renstrom, and C.E. Nichols, *The elongation behavior of the anterior cruciate ligament graft in vivo. A long-term follow-up study.* Am J Sports Med, 2001. **29**(2): p. 161-6.
 74. Butler, D.L., M.D. Kay, and D.C. Stouffer, *Comparison of material properties in fascicle-bone units from human patellar tendon and knee ligaments.* J Biomech, 1986. **19**(6): p. 425-32.
 75. Hamner, D.L., C.H. Brown, Jr., M.E. Steiner, A.T. Hecker, and W.C. Hayes, *Hamstring tendon grafts for reconstruction of the anterior cruciate ligament: biomechanical evaluation of the use of multiple strands and tensioning techniques.* J Bone Joint Surg Am, 1999. **81**(4): p. 549-57.
 76. Ishibashi, Y., T.W. Rudy, G.A. Livesay, J.D. Stone, F.H. Fu, and S.L. Woo, *The effect of anterior cruciate ligament graft fixation site at the tibia on knee stability: evaluation using a robotic testing system.* Arthroscopy, 1997. **13**(2): p. 177-82.
 77. Most, E., *Development of a 6-DOF Robotic Test System for Studying the Biomechanics of Total Knee Replacement*, in Dept of Mech Eng. 2000, Massachusetts Institute of Technology: Cambridge, MA.
 78. Zuppinger, H., *Die aktive Flexion im unbelasteten Kniegelenk.* Wiesbaden-Verlag von J. F. Bergmann, 1904.
 79. Morrison, J.B., *The mechanics of the knee joint in relation to normal walking.* J Biomech, 1970. **3**(1): p. 51-61.
 80. Menschik, A., *Mechanik des Kniegelenks, 1 Teil.* Z. Orthop, 1974. **112**: p. 481-495.
 81. Crowninshield, R., M.H. Pope, and R.J. Johnson, *An analytical model of the knee.* J Biomech, 1976. **9**(6): p. 397-405.
 82. Wismans, J., F. Veldpaus, J. Janssen, A. Huson, and P. Struben, *A three-dimensional mathematical model of the knee-joint.* J Biomech, 1980. **13**(8): p. 677-85.
 83. Essinger, J.R., P.F. Leyvraz, J.H. Heegard, and D.D. Robertson, *A mathematical model for the evaluation of the behaviour during flexion of condylar-type knee prostheses.* J Biomech, 1989. **22**(11-12): p. 1229-41.
 84. Blankevoort, L., J.H. Kuiper, R. Huiskes, and H.J. Grootenboer, *Articular contact in a three-dimensional model of the knee.* J Biomech, 1991. **24**(11): p. 1019-31.
 85. Blankevoort, L. and R. Huiskes, *Validation of a three-dimensional model of the knee.* J Biomech, 1996. **29**(7): p. 955-61.
 86. Trent, P.S., P.S. Walker, and B. Wolf, *Ligament length patterns, strength, and rotational axes of the knee joint.* Clin Orthop, 1976(117): p. 263-70.

87. Guo, X.E., *Mechanical Properties of Cortical Bone and Cancellous Bone Tissue*, in *Bone Mechanics Handbook*, S.C. Cowin, Editor. 2001, CRC Press: Boca Raton London New York Washington, D.C. p. 10.1-10.23.
88. Mommersteeg, T.J., L. Blankevoort, R. Huiskes, J.G. Kooloos, and J.M. Kauer, *Characterization of the mechanical behavior of human knee ligaments: a numerical-experimental approach*. J Biomech, 1996. **29**(2): p. 151-60.
89. Danylchuk, K., *Studies on the morphometric and biomechanical characteristics of ligaments of the knee joint*. 1975, University of Western Ontario: London, Ontario, Canada.
90. Girgis, F.G., J.L. Marshall, and A. Monajem, *The cruciate ligaments of the knee joint. Anatomical, functional and experimental analysis*. Clin Orthop, 1975(106): p. 216-31.
91. Li, G., J.F. Suggs, and T. Gill, *The Effect of ACL Injury on Knee Joint Function under Simulated Muscle Load*. Ann Biomed Eng, In press.
92. Li, G., S. Zayontz, E. Most, E. Otterberg, K. Sabbag, and H. Rubash, *The posterior cruciate ligament after total knee arthroplasty - a quantitative in-vitro investigation using robotic technology*. Submitted, 2001.
93. Kanamori, A., S.L. Woo, C.B. Ma, J. Zeminski, T.W. Rudy, G. Li, and G.A. Livesay, *The forces in the anterior cruciate ligament and knee kinematics during a simulated pivot shift test: A human cadaveric study using robotic technology*. Arthroscopy, 2000. **16**(6): p. 633-9.
94. Muellner, T., R. Reihnsner, L. Mrkonjic, W. Kaltenbrunner, O. Kwasny, R. Schabus, M. Mittlboeck, and V. Vecsei, *Twisting of patellar tendon grafts does not reduce their mechanical properties*. J Biomech, 1998. **31**(4): p. 311-5.
95. Clancy, W.G., Jr., D.A. Nelson, B. Reider, and R.G. Narechania, *Anterior cruciate ligament reconstruction using one-third of the patellar ligament, augmented by extra-articular tendon transfers*. J Bone Joint Surg Am, 1982. **64**(3): p. 352-9.
96. Bach, B.R., D.J. Daluga, R. Mikosz, T.P. Andriacchi, and R. Seidl, *Force displacement characteristics of the posterior cruciate ligament*. Am. J. Sports Med., 1992. **20**: p. 67-72.
97. O'Connor, J.J., *Can muscle co-contraction protect knee ligaments after injury or repair?* J Bone Joint Surg Br, 1993. **75**(1): p. 41-8.
98. Butler, J.C. and J.R. Andrews, *The role of arthroscopic surgery in the evaluation of acute traumatic hemarthrosis of the knee*. Clin. Orthop., 1988. **228**: p. 150-152.
99. Buckley, S.L., R.L. Barrack, and A.H. Alexander, *The natural history of conservatively treated partial anterior cruciate ligament tears*. Am. J. Sports Med., 1989. **17**: p. 221-225.
100. Noyes, F.R., P.A. Mooar, D.S. Matthews, and D.L. Butler, *The symptomatic anterior cruciate-deficient knee. Part I: the long-term functional disability in athletically active individuals*. J Bone Joint Surg Am, 1983. **65**(2): p. 154-62.
101. Ng, G.Y., B.W. Oakes, O.W. Deacon, I.D. McLean, and D. Lampard, *Biomechanics of patellar tendon autograft for reconstruction of the anterior cruciate ligament in the goat: three-year study*. J Orthop Res, 1995. **13**(4): p. 602-8.

102. Beynnon, B.D., R.J. Johnson, H. Toyama, P.A. Renstrom, S.W. Arms, and R.A. Fischer, *The relationship between anterior-posterior knee laxity and the structural properties of the patellar tendon graft. A study in canines.* Am J Sports Med, 1994. **22**(6): p. 812-20.
103. Ballock, R.T., S.L. Woo, R.M. Lyon, J.M. Hollis, and W.H. Akeson, *Use of patellar tendon autograft for anterior cruciate ligament reconstruction in the rabbit: a long-term histologic and biomechanical study.* J Orthop Res, 1989. **7**(4): p. 474-85.
104. Tohyama, H., B.D. Beynnon, R.J. Johnson, P.A. Renstrom, and S.W. Arms, *The effect of anterior cruciate ligament graft elongation at the time of implantation on the biomechanical behavior of the graft and knee.* Am J Sports Med, 1996. **24**(5): p. 608-14.
105. Lundberg, W.R., J.L. Lewis, J.J. Smith, C. Lindquist, T. Meglitsch, W.D. Lew, and B.C. Poff, *In vivo forces during remodeling of a two-segment anterior cruciate ligament graft in a goat model.* J Orthop Res, 1997. **15**(5): p. 645-51.
106. Beynnon, B.D., M.A. Risberg, O. Tjomsland, A. Ekeland, B.C. Fleming, G.D. Peura, and R.J. Johnson, *Evaluation of knee joint laxity and the structural properties of the anterior cruciate ligament graft in the human. A case report.* Am J Sports Med, 1997. **25**(2): p. 203-6.
107. Cain, T.E. and G.H. Schwab, *Performance of an athlete with straight posterior knee instability.* Am J Sports Med, 1981. **9**(4): p. 203-8.
108. Cross, M.J. and J.F. Powell, *Long-term followup of posterior cruciate ligament rupture: a study of 116 cases.* Am J Sports Med, 1984. **12**(4): p. 292-7.
109. Li, G., *Biomechanical Consequence of PCL Deficiency in the Knee under Simulated Muscle Loads - an in-vitro Experimental Study.* J Orthop Res, 2001. **In Press.**
110. Beynnon, B.D. and B.C. Fleming, *Anterior cruciate ligament strain in-vivo: a review of previous work.* J Biomech, 1998. **31**(6): p. 519-25.
111. Ishibashi, Y., S. Toh, Y. Okamura, T. Sasaki, and T. Kusumi, *Graft incorporation within the tibial bone tunnel after anterior cruciate ligament reconstruction with bone-patellar tendon-bone autograft.* Am J Sports Med, 2001. **29**(4): p. 473-9.
112. Li, G., O. Lopez, and H. Rubash, *Variability of a three-dimensional finite element model constructed using magnetic resonance images of a knee for joint contact stress analysis.* J Biomech Eng, 2001. **123**(4): p. 341-6.